



Cite this: *Nanoscale*, 2025, **17**, 14458

## Current state and potential of polymersomes as ocular drug delivery systems

Abuzer Alp Yetisgin, <sup>a,b</sup> Ponnurengam Malliappan Sivakumar<sup>c,d</sup> and Sibel Cetinel <sup>\*a,e</sup>

Amphiphilic copolymers can spontaneously form different structures such as micelles, worm-like micelles, and spherical and tubular polymersomes, determined by the ratio of hydrophilic and hydrophobic blocks. Among them, polymersomes are composed of an aqueous core and a hydrophobic membrane that can encapsulate hydrophilic and hydrophobic drugs. Significant effort has been dedicated to developing polymersomes for targeted delivery of drugs, particularly in cancer therapy. Nonetheless, polymersomes hold great potential for drug delivery to the ocular tissues as well. Polymersomes provide various advantages as ocular drug delivery systems due to their chemical and physical adaptability, ability to encapsulate multiple drugs, and precise control over parameters including size, shape, membrane characteristics, drug release, ability to traverse biological barriers, and responsiveness to stimuli. Despite the limited research to date, polymersomes, with their superior mobility within ocular compartments and their tunable properties, should be considered a promising option for ocular drug delivery, surpassing other vesicular systems such as liposomes and niosomes. In this review, we assessed the possibility of polymersomes as carriers for delivering drugs to ocular tissues.

Received 27th March 2025,

Accepted 23rd May 2025

DOI: 10.1039/d5nr01273b

rsc.li/nanoscale

### 1. Introduction

Two anatomical segments constitute the human eye: the anterior segment and the posterior segment.<sup>1,4</sup> The anterior segment comprises several parts such as the cornea, iris, conjunctiva, ciliary body, lens, lachrymal apparatus, and aqueous humor.<sup>5</sup> The posterior segment encompasses the vitreous humor, retina, choroid, sclera, and optic nerves.<sup>1,5</sup> Due to the complexity and vulnerability of ocular tissues to external injury, a strong defense mechanism consisting of numerous ocular barriers is required. Ocular barriers, which serve to protect the eye from potential damage, can be classified into three distinct categories: metabolic, dynamic, and static barriers. These include the blood-retinal barrier (BRB), corneal epithelium and stroma, lymphatic clearance, tear turnover, enzymes, and efflux pumps, among other essential

components.<sup>5–7</sup> Among these protective mechanisms, administering therapeutic doses of the drug to the posterior segment of the eye continues to be a major obstacle.

A substantial number of ocular conditions, although not generally viewed as life-threatening, severely impair the quality of life for affected individuals. Drugs have been produced with the intention of preventing and/or treating certain ocular disease.<sup>6,8</sup> However, the disease site bioavailability of commercial ophthalmic therapeutics is typically inadequate, requiring frequent administration.<sup>9</sup> Additionally, the route of drug administration differs based on the site of the disease. Systemic, topical, intravitreal, and subconjunctival routes are the most preferable methods of administration.<sup>1,5</sup>

Due to their substantial membrane thickness, precise drug release control, and capability to traverse biological barriers, vesicular nanocarriers, particularly polymersomes, have received significant interest in drug delivery.<sup>5,9,10</sup> Peptides, antibodies, proteins, enzymes, nucleic acids, and small molecules, regardless of the size, hydrophobicity or lipophilicity characteristics, have been encapsulated within polymersomes, which are alternatively referred to as polymeric vesicles. This property has made polymersomes focus in the development of drug carriers.<sup>11,12</sup> To tailor drug release, achieve targeted distribution, enhance bioavailability at specific sites, and protect drugs from degradation within the body, polymersomes offer versatile options for modifications, including adjustments to the size, surface properties, and composition.<sup>13</sup>

<sup>a</sup>Nanotechnology Research and Application Center (SUNUM), Sabanci University, Istanbul 34956, Türkiye. E-mail: [cetinel@sabanciuniv.edu](mailto:cetinel@sabanciuniv.edu)

<sup>b</sup>Faculty of Engineering and Natural Sciences, Sabanci University, Istanbul 34956, Türkiye

<sup>c</sup>Institute of Research and Development, Duy Tan University, Da Nang 550000, Viet Nam

<sup>d</sup>School of Engineering and Technology, Duy Tan University, Da Nang 550000, Viet Nam

<sup>e</sup>Faculty of Engineering and Natural Sciences, Molecular Biology, Genetics and Bioengineering Program, Sabanci University, Istanbul 34956, Türkiye



In an effort to improve drug bioavailability in the posterior segment of the eye by overcoming ocular barriers, a variety of drug formulations and extensive research have been done. Notably, the remarkable characteristics exhibited by polymerosomes, which encompass sustained and prolonged drug release, increased ocular retention, superior permeability, and flexible preparation processes, have made them an alternative drug delivery system. Recent research on the use of polymerosomes as potentially effective carriers for ocular drugs is the focus of this literature review. Moreover, an in-depth analysis is conducted on their methods of assembly and preparation, as well as the unique benefits they provide in terms of ocular application.

## 2. Requirements for ocular drug delivery

A combined research effort is needed to achieve the best ocular drug delivery system in the fields of pharmacokinetics (administration site, clearance, and bioavailability), drug potency (required concentrations at the target site), and formulation development (drug retention at the administrative site, payload, and release rate).<sup>14</sup> The eye's distinctive anatomy and physiological ocular barriers are major obstacles to the ocular drug delivery system (Fig. 1).<sup>15</sup> To bypass these barriers and reach the disease site, different routes of administration including topical, systemic, intracameral, subconjunctival, intravitreal, intraocular, retrobulbar, and juxtascleral.<sup>15,16</sup> The route of administration also depends on the type of diseases, such as posterior segment diseases (retinitis pigmentosa, diabetic retinopathy, diabetic macular edema, age-related macular degeneration, and choroidal neovascularization)<sup>17,18</sup> and anterior segment diseases (keratitis, anterior uveitis, conjunctivitis, glaucoma, corneal neovascularization, dry eye disease, and other ocular surface diseases).<sup>14,19</sup> In clinical practice, intravitreal injections are generally preferred for the treatment of diseases that impact the posterior segment.<sup>4,20</sup> By

use of these injections, which include the direct delivery of drugs into the vitreous humor, large drug concentrations can be delivered to the retina.<sup>9,21</sup> Patients often necessitate monthly or biweekly injections, as a result of existing dosing practices and the lack of sustained-release systems. Adherence to this frequent injection schedule significantly increases the tendency of patient noncompliance and inevitable complications following the administration, such as endophthalmitis, retinal toxicity, and retinal detachment.<sup>4,9</sup> As opposed to intra-vitreous route, topical administration offers a reduced risk of post-injection complications. However, due to ocular barriers, bioavailability of topical eye drop formulations are inadequate and constitute a field of constant development.<sup>4</sup>

### 2.1. Ocular barriers

Several physiological (nasolacrimal drainage, blinking), anatomical (dynamic and static), and metabolic (efflux pumps and enzymes) barriers delineate the reach of the drug to the targeted sites of the eye. The dynamic barriers include lymphatic clearance, tear turnover, and conjunctival blood flow, whereas the static barriers consist of the corneal stroma, stratified corneal epithelium, sclera, and other biological membranes.<sup>15,22</sup> These ocular barriers exert different effects on conventional drug delivery systems.

Ocular barriers can also be investigated under precorneal, corneal, and blood-ocular barriers. Precorneal barriers include the capacity of cul-de-sac and drug loss through lacrimal fluid as determining factors as well as corneal tear film. The average administration of eye drops to the cul-de-sac in humans is a maximum of 30  $\mu$ l. However, the cul-de-sac capacity is reduced up to 70–80% due to the lower eyelid movement to its original position. Pathological conditions such as inflammation and allergy also contribute to the reduction in cul-de-sac capacity. Thus, it regulates the drug concentration and acts as a precorneal barrier.<sup>23</sup> The loss of drugs through lacrimal fluid would happen due to non-productive absorption in conjunctiva, lacrimation, and solution drainage. The instilled drug solution (30  $\mu$ l) removed through lacrimal drainage until the tear reaches its original volume (7–9  $\mu$ l) leads to drug loss. Other factors, such as protein binding and the metabolism of drugs, also hinder drug absorption.<sup>16,23</sup> The goblet cells and other types of glands secrete the precorneal tear film, which has an 8  $\mu$ m thickness and acts as a barrier for drug absorption. It is a three-layered structure combined with mucin, an aqueous layer, and a lipid layer. The mucus layer part of the precorneal tear film forms a continuous fluid layer over the cornea and plays other roles such as maintaining moisture, preventing bacterial infection, removing foreign bodies, and providing lubrication for eyeball movement.<sup>24,25</sup> Due to the above reasons and the systemic absorption of drugs through conjunctiva, only less than 5% of drugs are absorbed when topical eye drops are instilled.<sup>24</sup> A detailed human tear film model proposed with different components such as the non-polar lipid sublayer and amphiphilic lipid sublayer (together form a lipid layer; ~40–90 nm thick layer), the aqueous-mucin gel layer (contains mostly water, carbohydrates, proteins, salt;

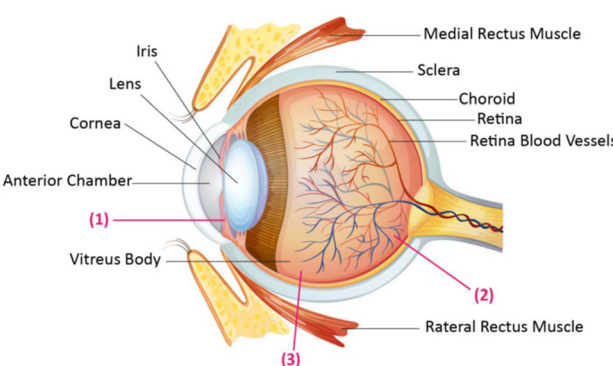


Fig. 1 Illustration of anatomy of the human eye and the routes of ocular drug delivery. (1) Topical route for eye drops, (2) systemic route through retinal capillaries, and (3) intravitreal drug injections (reprinted under terms of the CC-BY license from ref. 1. Copyright 2020, MDPI).



~4000 nm thick layer), the glycocalyx layer, and then the corneal epithelial cells will provide additional input in the design of ocular drugs.<sup>26</sup>

Structurally, the corneal surface is comprised of epithelium, stroma, and endothelium. The epithelium allows the passage of small and lipophilic molecules, whereas the stroma allows the passage of hydrophilic drugs. Endothelia provide selective permeability to hydrophilic drugs and macromolecules.<sup>23</sup> Hence, the cornea is a barrier to both hydrophilic and hydrophobic drugs due to its complex nature (the hydrophobic and hydrophilic natures of the epithelium and stroma, respectively). Thus, *trans*-corneal permeation is believed to be a rate limiting step in drug absorption from the lacrimal fluid to the aqueous humor. Researchers found that hydrophobic drugs were more permeable in the cornea compared to their hydrophilic counterparts. Nevertheless, less than 10% of the administered drug reaches the aqueous humor.<sup>27</sup> The conjunctiva is another barrier that is rich in vascularized tissue with abundant capillaries, and the drug absorption through blood vessels at the conjunctiva leads to drug loss into the systemic circulation.<sup>28</sup> The conjunctival route allows hydrophilic and large molecules (proteins and peptides) to be used in the absorption of biopharmaceuticals. However, this route is less relevant.<sup>25</sup>

There are two types of blood ocular barriers, namely, the blood-aqueous barrier and the blood-retinal barrier, where the former is present at the anterior part of the eye and the latter at the posterior part of the eye. The blood ocular barriers, like the blood brain barrier, protect the interior eye from drugs, macromolecules, and cells. The ocular barriers also prevent the entry and subsequent activity of systemic anti-inflammatory and antimicrobial drugs.<sup>29</sup> The blood-aqueous humor barrier is composed of the non-pigmented layer of ciliary epithelium, the posterior iridial epithelium, and the endothelium of iridial vessels.<sup>29</sup> The blood retinal barrier is composed of inner and outer parts, where the inner part is composed of tightly connected capillary endothelial cells that are covered by pericytes and Müller glial cells. Its role is to nourish the inner two-thirds of the retina and also intercept the seepage of plasma constituents to the retina.<sup>29,30</sup> Tightly connected retinal pigment epithelial (RPE) cells compose the outer blood retinal barrier. It maintains the integrity of the outer third of the retina and controls the blood supply to the photoreceptors from the choroid.<sup>29,30</sup>

## 2.2. Routes of administration

Topical drug delivery systems are meant to be used for localized and targeted drug delivery with minimal systemic side effects.<sup>31</sup> Hence, it remains suitable for the administration of beta-blockers, immunomodulatory agents, and several antimicrobial agents.<sup>32</sup> The delivery method is noninvasive, convenient, patient-compliance-oriented, and cost-effective; thus, more than 90% of conventional ocular products are delivered in the form of eye drops.<sup>15,32</sup> However, topical delivery of eye drops has several disadvantages, such as low bioavailability (<5%) due to lachrymation, precorneal loss factors, and tear

dynamics leading to frequent administration.<sup>15</sup> The ocular bioavailability can be improved by elevated pre-corneal retention time and enhanced permeation of drugs through corneal, scleral, and conjunctival routes.<sup>31</sup> Topical ointments, on the other hand, increase retention time but are associated with blurred vision, which reduces patient compliance.<sup>15</sup> Other approaches like therapeutic contact lenses, collagen corneal shields, prodrugs, non-aqueous formulations, penetration enhancers, penetrating peptides, and mucus osmotic particles have also been used to prolong the retention time and enhance permeation.<sup>31–33</sup> Engineered drug carriers such as liposomes, micelles, nano and microparticles also enhances the bioavailability and penetration of drugs.<sup>33,34</sup>

Intracameral injections are promising in the treatment of ocular hypertension, inflammation, infection, and neovascularization using drugs such as mydriatics, miotics, antiglaucoma, steroids, antibiotics, and anti-VEGF.<sup>35,36</sup> It delivers the drug directly to the anterior segment of the eye and ensures enhanced bioavailability, reduced corneal and systemic side effects, and lower ocular toxicity, which in turn outperforms the topical delivery.<sup>28,35</sup> On the other hand, toxic anterior segment syndrome, tissue hemorrhage, and toxic endothelial cell destruction syndrome are the major drawbacks associated with the intracameral route.<sup>28,31</sup>

Subconjunctival injection is used to deliver the drugs to the anterior and posterior segments of the eye. The typical injected volume is between 0.1 and 0.5 ml.<sup>14</sup> The majority of the subconjunctivally injected drugs are absorbed by the lymphatic system and blood circulation. Thus, the drug loss occurs through blood and lymphatic drainage *via* the conjunctiva.<sup>14,31</sup> Subconjunctival injections are less invasive than intravitreal, and self-assembled nanoparticles that are fabricated using gelatin-epigallocatechin gallate with or without a surface decorated with hyaluronic acid exhibit better delivery efficiency than topical eye drops.<sup>37</sup> It also achieves a high cell dose in low-volume solutions. Currently, in cell-based therapy, it is feasible to use subconjunctival injections to deliver mesenchymal stem cells (MSC) to treat the corneal failure occurring due to limbal stem cells deficiency and the technique is cost-effective since no substrata or surgical procedures are needed.<sup>38</sup>

Intravitreal injections (IVT) are preferred to directly deliver the drugs to the posterior part of the eye targeting the vitreous and retina, with an increasing application prevalence by 6% annually in the United States.<sup>15,39</sup> The major advantages include that IVT bypasses the blood-retinal barrier and corneal barriers.<sup>28</sup> IVT injections are frequently administered to achieve necessary therapeutic effects. However, these frequent administrations may cause poor patient compliance due to frequent clinic visits, and probable increased intraocular pressure, retinal detachment, endophthalmitis, and eyeball infection.<sup>31,40</sup> Although more than a million patients undergo IVT each year in Germany, a significant number of patients may have deprived themselves of therapy despite the significant benefits of the therapy.<sup>41</sup> Hence, an optimal protocol is to be established for IVT injections.<sup>31</sup>



The retrobulbar route delivers drugs to the retrobulbar space, which higher quantity of drug can be delivered with a maximum volume of 3–4 ml.<sup>24</sup> It has higher efficiency compared to the peribulbar route, which delivers the drug to the rectus muscles and their intramuscular septa.<sup>42</sup> Retrobulbar injections are considered a simple and safe procedure, but they are also classified as a blind procedure. Hence, there is a chance of injury to blood vessels, muscles, or the globe that cannot be entirely neglected. Thus, a surgeon with expertise is needed to prevent these complications.<sup>43</sup> This route is also suitable for local anesthetics and drugs like corticosteroids, chlorpromazine, and triamcinolone.<sup>24</sup>

Posterior juxtascleral injections are used in the treatment of some posterior segment complications and deliver drugs into the outer sclera surface.<sup>16,42</sup> This route can also achieve a higher drug concentration at the target site, which allows for higher drug penetration into the posterior parts of the eye. It also avoids the chances of intraocular damage and minimizes side effects like glaucoma, retinal detachment, and endophthalmitis. Drug efflux and systemic side effects are common; however, recent research and developments have addressed the drug efflux problem and increased drug efficiency. Similarly, systemic drug exposure is higher compared to intravitreal injections but much lower than systemic or topical routes.<sup>24</sup>

Recently, suprachoroidal injections have been used as a targeted drug delivery for the posterior segment of the eye and delivers the drug to the suprachoroidal space between the sclera and choroid.<sup>44</sup> It has advantages that include securing the delivery of immunogenic agents and larger biologicals.<sup>42</sup> Suprachoroidal space can be accessible with medical devices such as needles, microneedles, and catheters, whereas the use of microneedles results in more precise targeting and control than conventional hypodermic needles.<sup>44</sup> It is an invasive and complex route of administration, which may result in patient complications like hemorrhage and choroidal detachment.<sup>42</sup>

Lastly, the systemic route (parenteral and oral) of administration needs large doses to achieve the local effective drug concentration, which may lead to systemic side effects.<sup>40</sup> A systemic route can also be used to treat diseases in the posterior segment of the eye. However, only 1–2% of drugs manage to reach the vitreous cavity. Highly lipophilic molecules are selectively permeable to the blood-retinal barrier, which restricts the reach of the drug to the posterior segment of the eye. This route is considered to treat diseases like scleritis, episcleritis, and cytomegalovirus retinitis.<sup>31</sup>

### 2.3. Current approaches for overcoming ocular defence mechanisms

In topical delivery, the ocular bioavailability can be improved by elevated pre-corneal retention time and enhanced permeation through corneal, scleral, and conjunctival tissues.<sup>31</sup> Topical ointments increase retention time but are associated with blurred vision that reduces patient compliance.<sup>15</sup> Alternatively, addition of excipients such as viscosity modifiers, mucoadhesive polymers, and cyclodextrins, have been used to improve the pre-corneal retention time.

Nanotechnology-based drug delivery systems including liquid and semisolid formulations such as polymeric nanoparticles, lipid-based nanoformulations, and polymeric microparticles and solid formulations such as ocular inserts, collagen corneal shields, and contact lenses are also used to enhance the pre-corneal retention time and drug permeation.<sup>31,33,45</sup> Prodrugs, that are converted to their parent substances through chemical or enzymatic actions, are intended to be used for enhanced permeability, improved bioavailability, and extending the duration of action. For instance, ocular drugs with hydroxyl or carboxyl groups are esterified to convert into pro-ester drugs, which are lipophilic in nature. Pro-ester drugs can easily be activated in the corneal epithelium that produces esterase 2.5 times more than the stromal endothelium.<sup>46</sup> Non-aqueous eye drops also persist on the ocular surface for an extended duration because of their ability to incorporate into the lipid layer of tear film, immiscibility with tear fluid, and affinity towards corneal surface hydrophobicity.<sup>32</sup>

In ocular drug delivery, penetration enhancers are used to improve drug delivery through impermeable or limited permeable membranes. Their mode of action can be: (i) at the ocular surface, to modify the tear film stability and mucus layer; (ii) to alter the membrane lipid bilayers in epithelial cells; (iii) to slacken epithelial tight junctions. Cyclodextrins, chelating agents, crown ethers, surfactants, bile acids and bile salts, cell penetrating peptides (such as TAT, poly(arginine), penetratin, and low molecular weight protamine), and amphiphilic compounds are some of the penetration enhancers utilized in ocular drug delivery systems.<sup>47,48</sup> *In situ* gelling delivery systems have recently gained interest in ocular drug delivery. They are instilled as liquid that undergoes a phase transition to gel by the action of physiological stimuli such as pH, temperature, or ionic crosslinking. These gels exhibit enhanced local absorption and reduced pre-corneal elimination, which led to reduced systemic absorption and thus minimal side effects.<sup>49</sup>

Drug metabolism and stability of drug molecules are another aspect to be considered for better ocular delivery. Biomolecular drugs such as protein and peptides are easily degraded by the action of proteases and aminopeptidases, which reduces the bioavailability of these macromolecules. Endopeptidases such as collagenase and plasmin, which are present in the ocular tissues and fluids, may contribute to the degradation of proteins and peptides. One of the best examples is the hydrolytic degradation of peptides like methionine enkephalin and leucine enkephalin by aminopeptidase in rabbit corneal epithelium. However, methods such as glycoengineering, nanoparticles, liposomes, Fc-fusion, and PEGylation are used to protect the protein and peptide delivery, therefore increasing their therapeutic potential.<sup>50</sup> On the other hand, efflux proteins prevent the entry of antiglaucoma and antiviral drugs, while some of the metabolic enzymes prevent the entry of xenobiotics.<sup>15</sup> Drug efflux pumps of the ATP-binding cassette family (ABC), namely P-glycoprotein (ABCB1) and the multidrug-resistance-associated protein (MRP1; ABCC1), were found in ocular tissues. The former is found in the iris, cornea, and ciliary muscle, as well as in the

conjunctival epithelium, non-pigmented ciliary epithelium, and RPE, and it expels the drug from the retinal epithelial cells, whereas the latter is located on the choroidal side of the retinal barrier, which mediates the ATP-dependent transport of drugs and other xenobiotics.<sup>24</sup>

Nanoparticles provide distinctive advantages such as adhesiveness to prolong the drug residential and contact time,<sup>51</sup> penetration ability *via* surface engineering,<sup>52</sup> controlled (targeted/sustained) release by virtue of ocular microenvironment or external stimuli responsive particles,<sup>53</sup> and programmable propelling.<sup>54</sup> Among the properties of nanoparticles, particle size and surface charge (zeta potential) play a major role in ocular drug delivery, which determines the phagocytosis, distribution, and permeation of drugs. Particle sizes less than 200 nm are preferred and easily reach the anterior segments like cornea and conjunctiva. Scleral water channels and pores are between 30–350 nm.<sup>37,55</sup> Hence, hydrophilic particles with 20–80 nm can transit easily through these pores and reach to vitreous humor.<sup>55,56</sup> Cationic particles showed higher phagocytosis and internalization than those of anionic particles. The surface of the cornea and conjunctiva are negatively charged by nature, and the cationic particles undergo electrostatic interaction. This results in enhanced retention of the cationic nanoparticle at the anterior segment of the eye and improves drug delivery. However, the cationic nanoparticles are also fenced off at the lens and sclera because of their interaction with negative components like proteoglycans.<sup>57</sup> Similarly, cationic nanoparticles are able to interact with glycosaminoglycan and hyaluronic acid, which are negatively charged and present in the vitreous humor, which in turn hampers the diffusion, assists aggregation of the particle, and limits their retinal reach.<sup>58</sup> On the contrary, the anionic nanoparticles are able to reach the retina in injection form.<sup>37</sup> The nature of the particle and thereby their solubility and degradability are also to be considered in the design of ocular drug delivery. For instance, ocular tissues such as the cornea, sclera, vitreous, retinal pigment epithelium, and lens capsule are composed of fibrous, non-fibrous, and filamentous collagens.<sup>59</sup> Nanoparticles made up of collagen can be degraded *in vivo*, whereas its derivative, gelatin, is susceptible to proteolytic enzymes like papain, pepsin, chymotrypsin, and trypsin.<sup>60</sup> Similarly, chitosan, a cationic polymer, is degraded by lysozymes and chitinases to yield nontoxic glucosamine *in vivo*.<sup>61</sup> The vitreous body also contains hyaluronic acid and proteoglycans of chondroitin sulfate and heparin sulfate. These glycosaminoglycans can be broken down by hydrolases, such as heparin hydrolases, and lyases, such as hyaluronidase, chondroitinase, and heparinases.<sup>62</sup> Hence, they are biomimetic, biocompatible, biodegradable, and FDA-approved.

### 3. What are “polymersomes”?

#### 3.1. Discovery of polymersomes

Polymersomes, also known as polymeric vesicles, have been recognized for the past thirty years. Polymersomes are micro-/

nano-sized vesicles composed of a hydrophilic core surrounded by a hydrophobic membrane constructed from self-assembled amphiphilic copolymers, similar to liposomes.<sup>63,64</sup> Two publications were published in *Science* in 1995, which are among the first to discuss polymeric vesicles.<sup>65,66</sup> One study involved synthesizing amphiphilic polymers by combining polystyrene (PS) and poly(propylene) imine (PPI) dendrimers in different ratios. When self-assembled aggregates of these polymers were investigated under transmission electron microscopy (TEM), a variety of structures have been formed based on the number of amine head groups.<sup>65</sup> For instance, PS-dendr-(NH<sub>2</sub>)<sub>32</sub>, PS-dendr-(NH<sub>2</sub>)<sub>16</sub> and PS-dendr-(NH<sub>2</sub>)<sub>8</sub> amphiphilic copolymers self-assembled into spherical micelles, rod-like micelles, and spherical vesicles, respectively.<sup>65</sup> In the same year, Zhang and Eisenberg published their research on various morphological structures formed from PS-*b*-poly(acrylic acid) (PS-*b*-PAA) diblock copolymers in a water/*N,N*-dimethyl formamide (DMF) solution.<sup>66</sup> The morphologies varied according on the length of PAA chains, ranging from spherical micelles (26 nm, PS<sub>200</sub>-*b*-PAA<sub>21</sub>) to rod-like micelles (23 nm, PS<sub>200</sub>-*b*-PAA<sub>15</sub>) and vesicular structures (100 nm, PS<sub>200</sub>-*b*-PAA<sub>8</sub>).<sup>64,66</sup> These studies conclude that amphiphilic block copolymers are capable of forming aggregates with different shapes based on the hydrophobic-to-hydrophilic ratio. Discher *et al.* later showed that polymersomes generated from poly(ethylene oxide) (PEO)-poly(ethyl ethylene) (PEE) block copolymers were about ten times more durable than liposomes made from SOPC (1-stearoyl-2oleoyl phosphatidylcholine) phospholipids.<sup>67</sup> Tougher membranes of polymersomes can help protect drugs from dynamic barriers in the eye during topical distribution.

#### 3.2. Mechanisms of polymersomes self-assembly

Up to date, several polymersomes have been developed and analyzed. A critical packing parameter ( $p = \nu/a_0l_c$ ) is established as the primary design factor that influences the morphology of amphiphilic copolymer assemblies, where  $\nu$  is the volume of the hydrophobic part,  $a_0$  is the area of the hydrophilic part, and  $l_c$  is the length of hydrophobic part.<sup>68</sup> By controlling the critical packing parameter of amphiphilic copolymers, spherical micelles ( $p < 1/3$ ), cylindrical or rod-like micelles ( $1/3 < p < 1/2$ ), and spherical vesicles (polymersomes) ( $1/2 < p < 1$ ) have been formed, as seen in Fig. 2.<sup>68–70</sup> Additionally, in the cases of  $p = 1$  and  $p > 1$ , morphologies of planar lamellae and inverted structures have been generated.<sup>68,70,71</sup> Although the critical packing parameter is generally reliable, there can occasionally be aberrations in predicting the self-assembled structures of amphiphilic block copolymers.<sup>72</sup> In this regard, Discher *et al.* proposed utilizing the weight fraction of hydrophilic part ( $f_{\text{hydrophilic}}$ ) for determining the self-assembly of amphiphilic block copolymers.<sup>63</sup> If the hydrophilic fraction ( $f_{\text{hydrophilic}}$ ) is approximately  $35 \pm 10\%$ , amphiphilic copolymers can create polymersomes. If  $f_{\text{hydrophilic}}$  is less than 50%, cylindrical shaped aggregates might form. Polymeric micelles can be generated when the hydrophilic content exceeds 45% (Fig. 2).<sup>63,72</sup> The weight fraction



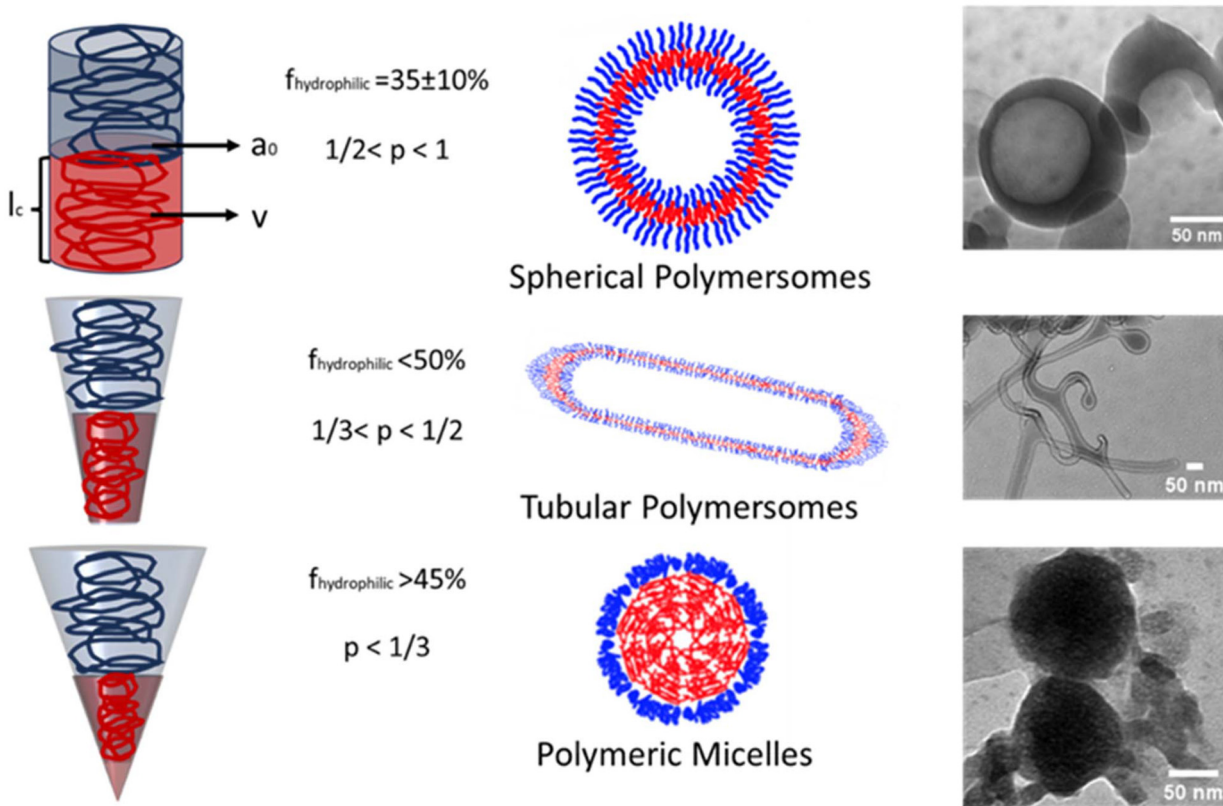


**Fig. 2** Illustration of critical packing parameter for determination of morphologies of polymeric assemblies and representative cryo-TEM micrographs of amphiphilic hyaluronan-based self-assemblies. For spherical polymersomes,  $f_{\text{hydrophilic}}$  equals to  $35 \pm 10\%$  or  $p$  between 0.5–1. For tubular polymersomes,  $f_{\text{hydrophilic}} > 50\%$  or  $p$  between 0.33–0.5. For polymeric micelles,  $f_{\text{hydrophilic}} > 45\%$  or  $p < 0.33$ .

ratio is limited to linear block copolymers, whereas the volume ratio of the hydrophilic component is appropriate for a broader range of amphiphilic copolymers, such as graft copolymers.<sup>73,74</sup> Nishimura *et al.* recently studied how structural control parameters affect the self-assembly of graft copolymers.<sup>73</sup> The study involved grafting poly(propylene oxide) (PPO), a hydrophobic group, onto three distinct hydrophilic main chains: dextran, poly(2-hydroxypropyl methacrylamide) (PHPMA), and mannan, all with similar degrees of substitutions (DS%). The study found that the morphology of polymeric self-assemblies was influenced by changing persistent length, which refers to the flexibility of the main polymer chain. With increasing persistent length among dextran < PHPMA < mannan, their *g*-PPO variants resulted in spherical micelles, rod-like micelles and polymersomes respectively.<sup>73</sup>

Self-assembly of amphiphilic polymers to polymersomes is driven by hydrophobic interaction *i.e.*, a type of noncovalent interaction, between hydrophobic fractions of block or graft copolymers in aqueous phase.<sup>13</sup> Hydrophilic fractions attract water molecules through hydration forces and operate as a barrier to prevent hydrophobic fractions from interacting with water molecules.<sup>13,72</sup>

Studies so far demonstrated two distinct mechanisms for polymersome formation, as seen in Fig. 3. Within mechanism I, also referred to as the bilayer-to-vesicle model, amphiphilic

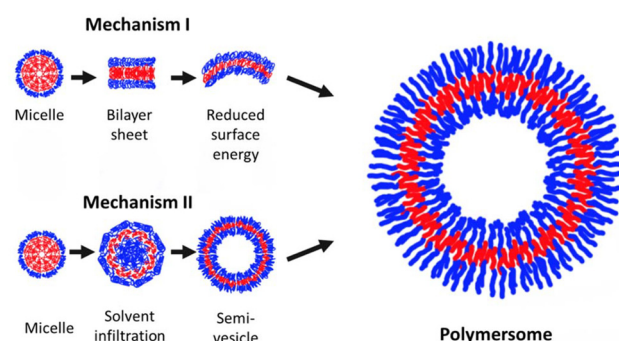


**Fig. 3** Illustration of proposed self-assembly mechanisms of amphiphilic copolymers into polymersomes (red indicates hydrophobic and blue indicates the hydrophilic blocks of the copolymers).

copolymers first form spherical micelles in aqueous solutions.<sup>75</sup> As the concentration of polymer in the solution increases, copolymers begin to transform into bilayer sheets. The decrease in surface energy eventually causes the bilayer sheets to close, resulting in the formation of polymersomes.<sup>13,72,75</sup> The mechanism I is a commonly acknowledged mechanism, supported by mathematical and experimental evidence.<sup>75,76</sup> On the other hand, in mechanism



II, spherical micelles first appear in the aqueous phase and then transform into semi-vesicles over time. The solvent diffuses due to decreasing bending energies caused by increasing curvature, leading to the formation of polymersomes.<sup>13,72</sup> Mechanism II was predicted using simulations of the external potential dynamics approach.<sup>13</sup>

### 3.3. Preparation methods of polymersomes

**Polymerization induced self-assembly (PISA).** Polymerization induced self-assembly (PISA) is a recently developed process utilized for generating polymersomes.<sup>77</sup> It is cost-effective and can be scaled up easily. The approach combines polymerization and self-assembly processes in a single stage.<sup>78,79</sup> The PISA approach permits the high-yield production of a variety of polymersomes at high concentrations.<sup>78</sup> The method employs differences in solubility between monomers and the copolymers which are synthesized in solution.<sup>80</sup> Commonly, reversible addition-fragmentation chain-transfer reaction (RAFT) method is used for polymerization of soluble homopolymer from first monomer. Homopolymer chain extension is then resumed with a second monomer that has low solubility in the solvent.<sup>78,80</sup> During the process, chain-extended copolymers progressively become insoluble.<sup>78,80</sup> Amphiphilic copolymer chains spontaneously convert into various structures such as micelles, worm-like micelles, and polymersomes to reduce the interfacial tension between the solvent and the part of the copolymer chain that is not soluble.<sup>78</sup> The shapes of self-assemblies can be influenced by the critical packing parameter, *p*, which is determined by the degree of polymerization (DP) of the hydrophobic and hydrophilic blocks of the amphiphilic copolymers.<sup>80,81</sup>

Polymersomes produced by the PISA method do not require additional processing. Instead, they may be tailored by modifying parameters including the degree of polymerization of both blocks, weight fractions of monomers, and the type of solvent. This makes the method advantageous and cost-effective. The PISA method's advantages are restricted by the synthesis of non-biodegradable polymersomes with the presence of (meth)acrylates and styrenic compounds, limiting their suitability for biomedical applications.<sup>78</sup> Recently, Zhang *et al.* demonstrated the effect of reaction temperature on the DP of PHPMA-poly(glycerol monomethacrylate) (PHPMA-PGMA) copolymer and polymersome morphologies *via* photo-PISA method.<sup>79</sup> At high reaction temperatures, membranes expanded both inward and outward during polymerization, resulting in increased size and thickness of polymersomes. Moreover, at lower reaction temperatures, polymersomes transformed into tubular and donut-shaped morphologies.<sup>79</sup> In another study, Varlas *et al.* prepared horse radish peroxidase (HRP) encapsulated and epoxy functionalized polymersomes *via* RAFT-mediated photo-PISA method from PEG, PHPMA, and poly(glycidyl methacrylate) (PGlyMA) (PEG<sub>113</sub>-*b*-P(HPMA<sub>320</sub>-*co*-GlyMA<sub>80</sub>)).<sup>82</sup> Polymersome membrane permeability is modulated using epoxide ring opening with diamine crosslinkers or hydrophobic amines.

The permeability decreased with increased membrane thickness compared to non-functionalized polymersomes.<sup>82</sup>

**Rehydration.** This approach is commonly utilized for preparing liposomes and has also been modified for producing polymersomes.<sup>64</sup> The process is considered as solvent-free, however it is still necessitating the use of organic solvents to dissolve both hydrophilic and hydrophobic blocks of the copolymers.<sup>64,69,83</sup> However, organic solvent is evaporated using a rotary evaporator or vacuum oven, leaving a thin layer of copolymers inside the container. An appropriate amount of aqueous solvent is dropped over the polymer films and vigorously mixed to form a dispersion, which triggers the self-assembly of polymersomes.<sup>64,69</sup> The rehydration process generates polymersomes with a wide size distribution. Therefore, an additional sonication, filtration, or extrusion steps are required to reduce the size and size distribution.<sup>80</sup> Xu *et al.* employed the thin film rehydration approach to produce paclitaxel (PTX) encapsulated PEG-*b*-PCL polymersomes.<sup>84</sup> The copolymers and PTX were dissolved in chloroform, an organic solvent, and a rotary evaporator was utilized to evaporate the solvent in order to produce a thin film of copolymers. Drug-loaded polymersomes with a size of 136.5 nm and an encapsulation efficiency (EE%) of 39.93% were self-assembled by rehydrating the thin film using sonication.<sup>84</sup> Some studies produced polymersomes using a direct hydration approach without the initial step of film preparation. Valvekar *et al.* developed vancomycin (VCM) loaded oleylamine-grafted hyaluronan (HA-OLA) polymersomes by directly hydrating bulk copolymers with probe sonication.<sup>85</sup> The size and encapsulation efficiency of HA-OLA polymersomes were below 250 nm and 43.12%, respectively.<sup>85</sup>

Greene *et al.* utilized the gel-assisted rehydration approach for producing polymeric giant unilamellar vesicles (GUVs) using poly(ethylene glycol)-poly(butadiene) (PEO-PBD) amphiphilic copolymers.<sup>86</sup> The size of polymeric GUVs was affected by temperature and the incorporation of membrane fluidizer molecules such as sucrose during the self-assembly process. Increasing the rehydration temperature considerably enlarged the polymersomes.<sup>86</sup> By slightly modifying the protocol of Greene *et al.*, recent study made by Tan, Schöller, and Ehmoser demonstrated rapid production of GUVs made from lipids and polymers (PEG-PLA) *via* agarose and PVA hydrogel-assisted rehydration methods by using multi-well plate.<sup>87</sup> The modified method will contribute to understanding GUV production and developing new platforms for ocular drug delivery.

**The solvent switch (solvent injection) method.** The solvent switch method is commonly utilized for producing polymersomes owing to its simplicity. Organic solvents including tetrahydrofuran (THF), dioxane, acetone, DMSO, or dimethylformamide (DMF) could be preferred to dissolve both hydrophilic and hydrophobic blocks of amphiphilic copolymers.<sup>68,78,88,89</sup> Organic solvent containing amphiphilic copolymers is gradually introduced into an aqueous solution, or an aqueous solution is introduced into the organic solvent.<sup>78,88</sup> The hydrophobic block of the amphiphile did not

dissolve in the aqueous solution, leading to self-assembly driven by interfacial tension between the membrane-forming polymer chains and the surrounding water. Finally, the organic solvent thoroughly removed from the solution *via* dialysis or evaporation.<sup>68,80</sup> Generated polymersomes often exhibit a wide size distribution, which might require post-processing methods to increase homogeneity.<sup>80</sup> The diameters and size distribution of polymersomes are influenced by the choice of organic solvent and the concentration of copolymers in the solvent. Wong *et al.* studied the self-assembly parameters of ellipsoidal PEG<sub>43</sub>-*b*-P(NIPAM<sub>21</sub>-*co*-PDMI<sub>9</sub>) (poly(ethylene glycol)-*b*-poly(N-isopropylacrylamide-*co*-perylene diester monoimide)) polymersomes *via* solvent switch method.<sup>90</sup> The study demonstrated that by adjusting the initial concentration of copolymers in THF and the final concentration in the aqueous phase, the shape and size of the particles could be shifted from small ellipsoidal micelles to large ellipsoidal polymersomes and from ellipsoidal to tubular polymersomes, respectively.<sup>90</sup>

**Nanoprecipitation.** Nanoprecipitation is similar to the solvent switch approach, with the main difference of rapid addition of the aqueous phase to the organic phase (or *vice versa*). When the mixing of the common and selective solvents occurs rapidly, the solvent quality deteriorates quickly to support copolymer rearrangement. Unlike the solvent switch method, where solvent addition is gradual and can take hours, this method involves rapid mixing, causing an abrupt loss in solvent quality.<sup>91,92</sup> As a result, the self-assembly process is effectively “frozen” before the copolymers can fully reorganize, leading to the formation of kinetically trapped polymersomes.<sup>93</sup> There are challenges associated with regulating self-assembly of copolymers including scalability, reproducibility, ease of fabrication, and loading efficiency.<sup>94</sup> The flash nanoprecipitation approach has been suggested for polymersome preparation for solving some of these issues, especially scalability.<sup>64,94</sup> In this process, a water-miscible organic solvent containing copolymers is rapidly mixed with an aqueous phase using multi-stream mixers under turbulent conditions. The resulting mixture is then transferred into an aqueous reservoir.<sup>64</sup> However, flash nanoprecipitation does not resolve the problem of low-concentration polymersomes due to the use of large reservoirs, making an additional concentration step necessary.<sup>64</sup> Alibolandi *et al.* demonstrated inhibitory effects of docetaxel (DTX) encapsulated and folate conjugated dextran-poly lactide-*co*-glycolide (Dex-PLGA) polymersomes, which prepared *via* nanoprecipitation, against human breast carcinoma (MCF-7) and mice mammary adenocarcinoma (4T1) cell lines.<sup>95</sup> The resulting polymersomes had a size of 178.5 nm, encapsulation efficiency of 78.85%, and drug loading capacity of 9.32%.<sup>95</sup>

**Microfluidics.** One of the latest techniques to produce polymersomes involves employing microfluidic devices to facilitate rapid self-assembly.<sup>80</sup> This method provides enhanced control over the self-assembly of polymersomes.<sup>96</sup> Microfluidics use a double emulsion system (w/o/w). Amphiphilic copolymers are dissolved in an organic solvent injected through the first

channel, while the aqueous phase (which may contain hydrophilic compounds) is injected through the second channel. This process leads to the formation of water-oil-in-water emulsions at the interface in the microchannels.<sup>80,97</sup> Polymersomes produced through this approach exhibit a narrow size distribution.<sup>98</sup> In addition, this method shows significant promise for the commercialization of polymersomes because of its suitability for large-scale production and reduction of batch-to-batch inconsistencies.<sup>93</sup> In a recent study, Wong *et al.* introduced a novel approach to generate polymersomes known as the continuous flow method. This method involved using micromixers to produce dynamic metastable polymersomes and incorporated downstream processes to control polymersome size and shape.<sup>99</sup> Thereby, the method offers scalability, a high polymersome production rate (over 3 g h<sup>-1</sup>), method robustness, suitability for different copolymers, and a plug-and-play production setup.<sup>99</sup> Martin *et al.* produced polymersomes by utilizing PEG-*b*-PTMC (PEG-*b*-poly(trimethylene carbonate)) diblock copolymers through a microfluidic method.<sup>100</sup> The study on microfluidic chips (micromixer and herringbone) with different flow regimes found no significant differences in the fabricated polymersomes. The concentration of copolymer influenced the size of polymersomes, which ranged from 76 nm to 224 nm as the concentration increased from 0.2 mg mL<sup>-1</sup> to 6 mg mL<sup>-1</sup>.<sup>100</sup> In addition, the polymersomes’ size increased from 160 nm to 218 nm by reducing the flow rate from 1000 µL min<sup>-1</sup> to 100 µL min<sup>-1</sup>.<sup>100</sup>

**Electroformation.** Electroformation is a solvent-free method that is derived from film rehydration and could also be referred to as the aided-film rehydration method.<sup>78,80</sup> Electroformation has been employed in the preparation of GUVs.<sup>68</sup> In brief, the amphiphilic copolymer film is deposited onto electrodes—such as gold, indium-titanium oxide (ITO) glass, or platinum—by dissolving it in a volatile organic solvent, applying the solution to the electrodes, and allowing the solvent to evaporate.<sup>69,80</sup> Afterwards, an alternating current (AC) is used to apply to the electrodes in order to regulate the rate of water diffusion across the copolymer film.<sup>69</sup> As a result of controlled extend of bulging and separation between vesicular structures, polymersomes with precise size distributions are generated.<sup>80</sup> Previously, giant unilamellar vesicular (GUV) polymersomes made of poly(ethylene oxide)-*b*-poly(butadiene) (PEO<sub>13</sub>-PDB<sub>22</sub>) were produced using electroformation method.<sup>101</sup> It’s reported that nanosecond electrical pulses with varying repetition rates and buffer solutions with different conductivities impact the size and shape of polymersomes. Additionally, the polymersomes at concentrations up to 250 µg mL<sup>-1</sup> exhibit no cytotoxic effects on Chinese hamster ovary (CHO) and B16-F1 murine melanoma cells for 48 hours.<sup>101</sup>

### 3.4. Optimization of polymersomes and post-processing methods

Considering the production method used, several factors affect the properties of polymersomes. To obtain an optimal poly-



mersome formulation, these factors should be investigated individually. In most cases, the type of organic solvent, the size and ratio of hydrophilic to hydrophobic blocks of the amphiphilic polymers, and the polymer concentrations are the major influencing factors.<sup>102,103</sup> A study proposed a modified solvent switch approach for the rapid and straightforward formation of polymersomes using different block copolymers.<sup>103</sup> Accordingly, the size of polymersomes are modified by adjusting a few preparation factors such as the temperature during THF evaporation, aging of polymersomes in a mixed solvent, lengths of hydrophilic–hydrophobic blocks of copolymers, and the ionic strength of the aqueous solution.<sup>103</sup> Polymersomes that are composed of the same block copolymers with diameters between 200 nm and 2  $\mu$ m are produced using this technique.<sup>103</sup> In another study, Sanson *et al.* addressed the factors influencing the size and size distribution of polymersomes produced *via* nanoprecipitation method.<sup>104</sup> The nanoprecipitation parameters, such as copolymer concentration, organic solvent type, duration, and order of solvent addition (aqueous-to-organic or organic-to-aqueous), influence the assembly of poly(trimethylene carbonate)-*b*-poly(L-glutamic acid) (PTMC-*b*-PGA) diblock copolymers into polymersomes with various sizes.<sup>104</sup> Increased copolymer concentration has been demonstrated to increase the size of polymersomes. The size of polymersomes are increased with prolonged injection rates as well.<sup>104</sup> In case of microfluidics method, the size of polymersomes can be regulated by adjusting the flow rate ratios of solvents.<sup>80</sup> Producing smaller sized polymersomes requires using a higher flow rate ratio of solvents and smaller channel widths.

Many polymersome preparation techniques lead to a mixture of polymersomes with different sizes and structures. Therefore, post-processing techniques may be utilized to separate the preferred polymersome fraction. Different approaches such as extrusion, gel permeation chromatography, centrifugation, sonication, and freeze–thaw cycles are employed for modifying the size of polymersomes.<sup>64,69</sup> Moreover, purification procedures including dialysis and centrifugation are necessary to remove residual organic solvent.<sup>13,97</sup> Residual organic solvents may lead to toxicity in both *in vitro* and *in vivo* experiments and hinder biomedical uses. Organic solvents can function as plasticizers, reducing the membrane stability of polymersomes in the solution.<sup>64</sup> Men *et al.* established post-processing methods for obtaining polymersomes with smaller sizes (<100 nm) by utilizing organic solvent as a plasticizer in extrusion and sonication processes.<sup>105</sup> When the organic solvent ratio in the solution was 66.7 v/v% (water content of 33.3 v/v%), the size of PEG-*b*-PS (PEG-*b*-polystyrene) polymersomes were reduced to 100 nm or lower with a uniform size distribution upon 30 seconds of sonication.<sup>105</sup> When water percentage increased to 50 v/v% and sonication time to 5 minutes, only a portion of the polymersomes' sizes were reduced. Meanwhile, the membranes exhibited increased rigidity as the water content increased to 66.7 v/v%.<sup>105</sup>

### 3.5. Encapsulation methods

As many self-assembled vesicular particles, polymersomes have the ability to encapsulate hydrophilic, hydrophobic, and amphipathic compounds.<sup>92,106</sup> In addition, polymersomes provide the option to load either single or multiple drug molecules per polymersome using different methods, *etc.* active and passive loading or covalent attachment of drug molecules.<sup>107</sup> Hydrophilic drugs are frequently contained in an aqueous core, whereas hydrophobic molecules are kept within the membranes of polymersomes.<sup>108</sup>

Passive and active loading methods are generally preferred for encapsulation of hydrophilic drugs to polymersomes. Passive loading refers to the simultaneous encapsulation of drug molecules in the aqueous phase during the preparation of polymersomes.<sup>109</sup> A defined amount of drug is dissolved in the aqueous phase and then added to the organic phase during the preparation process.<sup>110–112</sup> Active (remote) loading methods involve transmembrane gradients including pH and salt depending on drug properties, such as ionizability and diffusivity across polymeric membranes. This approach is particularly effective for low molecular weight drugs and slightly polar weak acids/bases.<sup>64,107,109</sup> Thicker membranes are beneficial for facilitating rapid diffusion of drugs during active loading.<sup>109</sup> The transmembrane pH gradient method relies on the ionization of basic drug molecules and their penetration into the acidic core of polymersomes.<sup>113</sup> In the transmembrane ion gradient method, phosphate or sulfate salts are used for loading drug molecules.<sup>114</sup> In most cases, following these drug loading strategies, any remaining drugs are removed from polymersome solutions through dialysis or centrifugation.<sup>111,113,114</sup> Maintaining the integrity of membranes is crucial for active drug loading strategies, as compromised membranes can result in poor encapsulation efficiencies and premature drug release.

Hydrophobic drugs are frequently enclosed within the bilayer of polymersome membranes through passive encapsulation. Organic phase dissolves hydrophobic drugs and encapsulates them in polymersomes through the self-assembly process.<sup>115,116</sup> Polymersomes have thicker membranes, typically ranging from 5 to 50 nm, in contrast to liposomes that have membrane thicknesses ranging from 3 to 5 nm. This feature is highly advantageous for encapsulating hydrophobic drugs.<sup>69,96,109</sup> Moreover, the increased thickness of polymersomes leads to a longer diffusion distance, which results in a decrease in drug release rates.<sup>69</sup> A prior study evaluated the consequences of encapsulating a hydrophobic small molecule, bromoindirubin-3'-oxime, in the core or membrane of polymersomes.<sup>117</sup> Encapsulation of drug to either side yielded an efficiency of approximately 90%. In addition, the hydrodynamic sizes and PDI values showed similar results at the initial measurements. Following a 14-day period, there was a notable increase in size and PDI values of aqueous core encapsulated polymersomes compared to membrane loaded polymersomes indicating a more stable particle generation with hydrophobic drugs loaded to the membrane.<sup>117</sup>

Besides drug encapsulation, various compounds such as peptides, lipids, antibodies, and small drugs can be attached to amphiphilic copolymer chains to target disease sites and evade the immune system.<sup>85,109,118-120</sup> Conjugation amount might be restricted by the critical packing parameter of amphiphilic copolymers, which plays a crucial role in determining the morphology of polymersomes.

### 3.6. Drug release and stimuli-responsive polymersomes

Understanding the drug release rates of both hydrophilic and hydrophobic drugs is essential when evaluating drug carrier systems.<sup>121</sup> Drug molecules might be released rapidly from nanocarriers before reaching the intended site. As a result, the rapid elimination and breakdown of drug molecules or side effects on healthy tissues may drastically reduce the effectiveness of the treatment.<sup>106</sup> One potential solution to the problem involves attaching drug molecules to amphiphilic copolymers using biodegradable linkers to enhance drug retention in the polymersomes.<sup>109,122</sup> When there is a need for fast drug release, the membrane of polymersomes can be assembled from biodegradable polymers including polysaccharides, polypeptides, polyesters, and polycarbonates.<sup>121</sup> On the other hand, drug release could be directed by responding to internal and external stimuli, which could impact properties including membrane permeability or polymersome breakdown.<sup>92,123,124</sup> Various chemical and physical factors such as pH, temperature, ultrasound, light, enzymes, ionic gradient, and redox potential could play a role in releasing drugs at the desired site of action.<sup>124,125</sup> For instance, polymersomes composed of hyaluronic acid-*b*-poly (β-amino ester) (HA-PBAE) diblock copolymers were developed to encapsulate DOX for treating metastatic breast cancer.<sup>126</sup> The hyaluronan part of the copolymer targeted the CD44 receptors present on breast cancer cells. At a pH of 5.5, the hydrophobic nature of PBAE blocks shifted to hydrophilicity as a result of the protonation of amine groups.<sup>126</sup> Thereby, the release of DOX was improved through disrupted polymersome membranes.<sup>126</sup> In a different study, Ferrero *et al.* developed redox-responsive MPEG-PDH-mPEG polymersomes and loaded them with DOX.<sup>127</sup> This tri-block copolymer consists of PEG methyl ether hydrophilic blocks and a hydrophobic block with disulfide bounds. Polymersomes containing drugs showed an encapsulation efficiency of 98% with approximately 34% of DOX being released within 48 hours.<sup>127</sup> Upon the addition of 50 mM glutathione (GSH) the drug release rate was doubled, resulting in the release of approximately 77% of the drug due to the cleavage of disulfide bonds.<sup>127</sup>

## 4. Polymersomes as drug carriers

Polymersomes are made up of an aqueous core and a dense hydrophobic membrane, allowing them to enclose hydrophilic, lipidic, and amphiphilic molecules (Fig. 4).<sup>92,128</sup> Consequently, polymersomes with dual therapeutic formulations can allow novel theranostic strategies for simultaneous

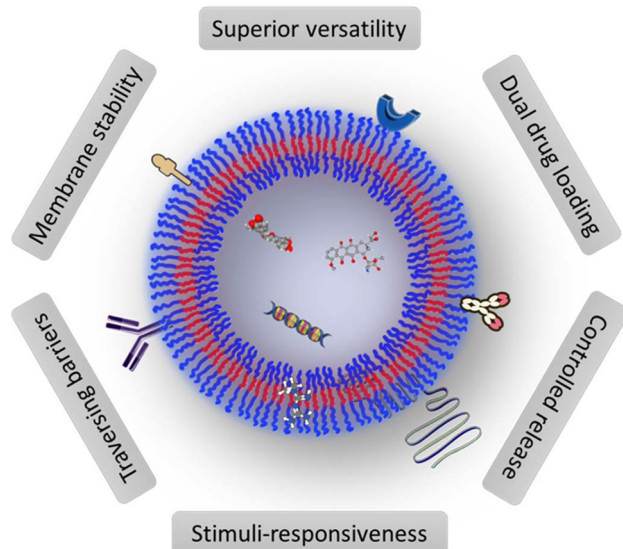


Fig. 4 Schematic representation of polymersomes with advantages including superior physical and/or chemical versatility, dual loading of hydrophilic and hydrophobic drugs, high control over release kinetics, stimuli-responsive drug delivery, strong potential to traversing biological barriers, and a highly stable membrane structure.

detection and treatment of the diseases. Zavvar *et al.* synthesized theranostic PEG-PCL polymersomes containing indium-copper-gadolinium-zinc sulfide hydrophobic quantum dots as contrast agents for magnetic resonance (MR) – fluorescence imaging, in combination with doxorubicin (DOX) for breast cancer treatment.<sup>129</sup> Additionally, the polymersomes' surface was modified using AS1411 DNA aptamer to provide targeted delivery of drugs.<sup>129</sup> These targeted polymersomes were delivered to the tumor site and detected at the tumor location using MR imaging 24 hours after injection. Drug-loaded polymersomes effectively reduced tumor growth in BALB/c mice.<sup>129</sup> D'Angelo *et al.* produced PEG-PCL polymersomes to encapsulate two cancer therapeutics: doxorubicin (DOX) and vemurafenib (VEM).<sup>130</sup> Highly stable dual drug loaded polymersomes were produced with encapsulation efficiencies of 55% for VEM and 39% for DOX.<sup>130</sup> Dual contrast agents can also be added to polymersomes to improve diagnostic imaging. Gadolinium cations and Cy5.5 were included into self-assembled poly(acrylic acid-*co*-distearin acrylate) polymersomes, resulting in improved contrast both in near-infrared (NIR) and magnetic resonance (MR) imaging.<sup>131</sup>

Capsosomes and PICsomes (polyion complex vesicles) are relatively new types of polymersomes. Capsosomes are nanocarrier systems that consist of liposomal sub-compartments enclosed by polymeric membranes.<sup>106</sup> Capsosomes are generally produced by sequentially depositing liposomal and polymeric membranes onto sacrificial nanoparticles that act as a template.<sup>106</sup> Yoo *et al.* constructed capsosomes by integrating hyaluronic acid and chitosan coating on cationic liposomes as the core using a layer-by-layer technique resulting in sizes between 500 nm to 2 μm.<sup>132</sup> PICsomes, on the other hand, are



formed by mixing oppositely charged copolymers in an aqueous phase.<sup>106</sup> PICsomes demonstrated high physiological stability, even with the media that contains serum proteins.<sup>133</sup> Recently, Aydinlioglu *et al.* made robust PICsomes from PEO-*b*-poly(amino acids) complexes which were assembled at near charge equilibrium and successfully encapsulated small interfering ribonucleic acid (siRNA).<sup>12</sup>

Polymersomes demonstrate preferable durability, a wide variety of customization options, and enhanced membrane stability in comparison to liposomes, niosomes, micelles, or nanogels.<sup>92,109</sup> Polymersomes could be tailored in terms of size, surface potential, membrane thickness and permeability, biodegradability, and stimuli-responsiveness to fulfill specific application demands.<sup>120,134,135</sup> Additionally, the surface of polymersomes can be readily decorated with various kinds of targeting molecules including peptides, growth factors, antibodies, and proteins.<sup>83,136</sup> Polymersomes can also be assembled directly from polysaccharides or proteins with inherent targeting properties, such as hyaluronan (HA), collagen, gelatin, and chondroitin sulfate (CS).<sup>83,118,137</sup> Besides, polymersomes possess an innate targeting mechanism that sets them apart from liposomes and niosomes.

Noteworthy to mention that the polymersomes have promising potential to traverse biological barriers.<sup>138,139</sup> Recently, sphingosine-grafted HA polymersomes reached to the retina of the porcine eyes by passively traversing biological barriers including BRB, when applied topically in an *ex vivo* study.<sup>3</sup> In another study, Joseph *et al.* observed that asymmetrical polymersomes made from mixing poly(ethylene oxide)-poly(butylene oxide) (PEO-PBO) copolymer with either poly[(2-methacryloyl)ethyl phosphorylcholine]-poly[2-(diisopropylamino)ethyl methacrylate] (PMPC-PDPA) or poly[oligo(ethylene glycol) methyl methacrylate] (POEGMA)-PDPA copolymers can actively traverse blood-brain barrier (BBB) by chemotaxis.<sup>140</sup> The chemotaxis of asymmetrical polymersomes was achieved by incorporating glucose oxidase and/or catalase into polymersomes to propel toward high glucose concentrated regions.<sup>140</sup> Moreover, the chemotactic polymersomes combined with low-density lipoprotein receptor-related protein 1 as targeting moiety to achieve 4-fold increased penetration of BBB, compared to non-chemotactic polymersomes.<sup>140</sup> Shao *et al.* demonstrated that photoactivable nanomotors based on gold-coated poly(ethylene glycol)-*b*-poly(D,L-lactide) (PEG-PDLLA) polymersomes (size <200 nm at pH 7.4) were able to traverse biological membranes to deliver drugs to tumor.<sup>141</sup>

On the other hand, there are certain concerns regarding the biomedical applications of polymersomes notwithstanding their advantages. Polymersomes that are composed of non-biodegradable polymers and/or degradation products of some biodegradable polymers could be undesirable due to the possible toxicity of by-products in a dose-dependent manner.<sup>64</sup> The data on safety profiles of polymersomes are limited due to the lack of pre-clinical and clinical research. Polymersomes produced from polymers which are approved by the FDA could potentially resolve this problem. Additionally, scaling-up the production of polymersomes is another issue to address for

commercialization, due to similarity of production methods with liposomes which also face the issue.<sup>64</sup>

## 5. Ocular drug delivery with polymersomes

Research studies on ocular drug delivery have primarily concentrated on the use of nanocarriers including liposomes and niosomes. However, recent studies have highlighted the significant potential of polymersomes in ocular drug delivery (Table 1). Especially, the comparative studies made by Ridolfo *et al.* who analyzed the drug release kinetics and vitreous mobility of polymeric micelles and polymersomes with different sizes and shapes, including spherical and tubular polymersomes, as well as spherical and worm-like micelles.<sup>142</sup> The micelles were formed using copolymers of poly(ethylene glycol) (PEG) as hydrophilic block with different combinations of poly(trimethylene carbonate) (PTMC) and poly( $\epsilon$ -caprolactone) (PCL) as the hydrophobic blocks. Meanwhile, spherical and tubular polymersomes were produced from PEG and poly(D,L-lactic acid) (PDLLA).<sup>142</sup> Polymersomes encapsulating dexamethasone (DEX), were prepared *via* solvent switch method, while micelles were formed through direct hydration. Vitreous mobility was further assessed in terms of surface functionalization with either amine or carboxylic acid-modified PEG. Among all formulations, worm-like micelles exhibited the highest drug loading capacity (10 wt%), followed by spherical micelles (4 wt%) and polymersomes (0.5 wt%).<sup>142</sup> This difference in drug loading efficiency was expected considering hydrophobic nature of DEX and high aspect ratio of worm-like micelles. Interestingly, cellular uptake studies with retinal pigment epithelial (ARPE-19) cells revealed that high-aspect ratio particles (tubular polymersome or worm-like micelles) internalized more efficiently by the cells than their spherical counterparts. Moreover, high-aspect ratio particles demonstrated greater vitreous mobility than spherical particles.<sup>142</sup> Tubular polymersomes exhibited 55%–75% higher mobility than spherical polymersomes, suggesting that shape plays a crucial role in diffusion through the vitreous. In addition, surface modifications influenced vitreous mobility, whereas carboxylic acid modified self-assemblies demonstrating increased mobility, potentially due to the electrostatic interactions with hyaluronic acid in the vitreous. However, the vitreous mobility of tubular polymersomes was slower compared to worm-like micelles.<sup>142</sup> Building upon these findings, Junnuthula *et al.* studied the *in vivo* ocular pharmacokinetics of polymersomes and polymeric micelles, which were assembled from poly(ethyleneglycol)-*b*-poly( $\epsilon$ -caprolactone)-*g*-poly(trimethylene carbonate) and poly(ethylene glycol)-*b*-poly(trimethylene carbonate), respectively.<sup>143</sup> Polymersomes (~100 nm) and micelles (~30 nm) were administered into the rabbit eyes *via* intravitreal injections, revealing significant differences in retention times. Polymersomes exhibited prolonged half-lives in the vitreous (11.4–32.7 days) compared to micelles (4.3–9.5 days), with intravitreal clearance values of

**Table 1** Summary of studies that utilized polymersomes for ocular drug delivery

Hydrophilic part	Hydrophobic part	Drug	Results	Ref.
PEG	PDLLA	DEX	Tubular polymersomes had better vitreous mobility and cellular uptake than spherical ones.	142
PEG	Poly( $\epsilon$ -CL- <i>g</i> -PTMC)	—	Polymersomes (~100 nm) had longer vitreous half-lives (11.4–32.7 days) and slower clearance compared to micelles.	21
mPEG	Cholesterol or cholane	ML240	Retinal neuroprotection >21 days after single administration.	145
PEO	PPO	CF and VP	Lipo-polymersomes achieved 92.8% EE, 99% glioblastoma cell viability reduction after irradiation.	146
PGMA and PDMAPM	PDMS	Cur	Self-healable antimicrobial hydrogels were developed as potential antimicrobial contact lenses. Inhibition against <i>E. coli</i> and <i>S. aureus</i> .	147
PEGMA- <i>co</i> -PBA	PMTEMA	CIP	ROS-responsive polymersomes improved antibacterial efficacy and corneal retention for bacterial keratitis.	2
HA	Sph	Sph	Topically applied polymersomes reached retina in 24 h. Inhibited tube formation selectively without harming ARPE-19.	3

1.7–8.7  $\mu\text{L h}^{-1}$  and 3.6–5.4  $\mu\text{L h}^{-1}$ , respectively.<sup>143</sup> It is worth mentioning that polymersomes remained detectable in the vitreous after 92 days post-injection, and were found to accumulate at the optic nerve head by day 111, further underscoring their potential for long-term drug delivery to the posterior segment of the eye.<sup>143</sup> In a comparative study, Amir Sadeghi *et al.* evaluated the *in vivo* ocular pharmacokinetics of polymeric micelles (PEG-*b*-PTMC, 37.5 nm) against liposomes (48.6 nm).<sup>144</sup> Their results showed that both liposomes with size ~50 nm and polymeric micelles with size <90 nm were retained for 10–65 days in the vitreous of rats, while liposomes ~1000 nm persisted for at least 20 days. The prolonged retention of larger liposomes was attributed to the 550 nm mesh size of the vitreous, which may impede the diffusion.<sup>144</sup> These comparative studies demonstrated that, in terms of vitreous mobility, retention time, and prolonged drug release, polymersomes (both tubular and spherical) are superior alternatives to micelles or liposomes. Nevertheless, the choice between micelles and polymersomes should be carefully made based on the administration route, drug type, required retention and release profiles, and the target ocular tissue.

Other than comparative studies, a few studies were utilized the polymersomes as ocular drug delivery systems. Recently, polymersomes have demonstrated potential for retinal neuroprotection. Self-assembled polymersome-like particles were generated by Sen *et al.* using mPEG-Chol (methoxy-poly(ethylene glycol)-cholesterol) and mPEG-cholane amphiphilic polymers using a rehydration method.<sup>145</sup> These particles encapsulated ML240, an inhibitor targeting ATP-driven chaperone valosin-containing protein (VCP). The results of *in vivo* studies presented the retinal neuroprotective activity of ML240-loaded particles for longer than 21 days.<sup>145</sup> On the other hand, de Oliveira *et al.* took another approach and combined liposomes with amphiphilic polymers to develop lipo-polymersomes.<sup>146</sup> They proposed verteporfin (VP)-loaded and 5(6)-carboxyfluorescein (CF) conjugated lipo-polymersomes for photodynamic therapy (PDT) in ocular tissues.<sup>146</sup> The lipo-polymersomes, composed of DPPC (1,2-dipalmitoyl-*sn*-glycero-3-phosphatidylcholine) as phospholipid and Pluronic® F127 (PEO<sub>106</sub>-PPO<sub>70</sub>

PEO<sub>106</sub>) as amphiphilic polymer, were produced using film rehydration method.<sup>146</sup> These lipo-polymersomes with size of 112.1 nm and zeta potential of 0.97 mV, exhibited a high encapsulation efficiency of 92.8%. Furthermore, upon irradiation with a blue LED (6.62 J cm<sup>-2</sup>), drug loaded lipo-polymersomes achieved 99% reduction in T98G glioblastoma cell viability, indicating their potential in targeted ocular PDT.<sup>146</sup> Considering the structure of their lipo-polymersomes, it is more closely related to a liposome than a polymersome; however, this study demonstrated that it is possible to combine the advantages of both nanocarriers rather than choosing one over the other. Banerjee *et al.* developed a self-healable, antifouling PDMS-based hydrogel incorporating curcumin (Cur)-loaded zwitterionic PDMS polymersomes for potential use in contact lenses.<sup>147</sup> The hydrogel was prepared from crosslinking of PEG-DA (polyethylene glycol dialdehyde) and amine functionalized PDMS polymersomes, which was composed of poly(glycidyl methacrylate)-block-polydimethylsiloxane-block-poly(glycidyl methacrylate) (PGMA-*b*-PDMS-*b*-PGMA) triblock copolymer *via* RAFT polymerization and Schiff-base reaction.<sup>147</sup> Moreover, Cur-loaded zwitterionic PDMS polymersomes, composed of poly(*N*-[3-(dimethylamine)propyl]methacrylamide) and PDMS (PDMAPM-*b*-PDMS-*b*-PDMAPM) were incorporated into hydrogels to make them antimicrobial.<sup>147</sup> Both polymersomes exhibited a broad size distribution with similar sizes. The zwitterionic polymersomes were measured around  $282 \pm 4$  nm in size with a PDI of 0.379, while the amine-functionalized polymersomes had a size of  $255 \pm 5$  nm and a PDI of 0.334. Moreover, Cur-loaded polymersomes exhibited an encapsulation efficiency of 63.4% and a loading capacity of 4.2%.<sup>147</sup> The hydrogel was biocompatible for HaCaT cells and human dermal fibroblasts at concentrations up to 50  $\mu\text{g mL}^{-1}$ .<sup>147</sup> Notably, it exhibited antimicrobial effects against both Gram-negative (*E. coli*) and Gram-positive (*S. aureus*) bacteria, demonstrated by inhibition zones of  $17 \pm 1.5$  mm and  $14 \pm 0.5$  mm, respectively.<sup>147</sup> These findings suggest that polymersome-integrated self-healable hydrogels could serve as ocular lenses with antimicrobial and therapeutic effects. Furthermore, it may be possible to develop



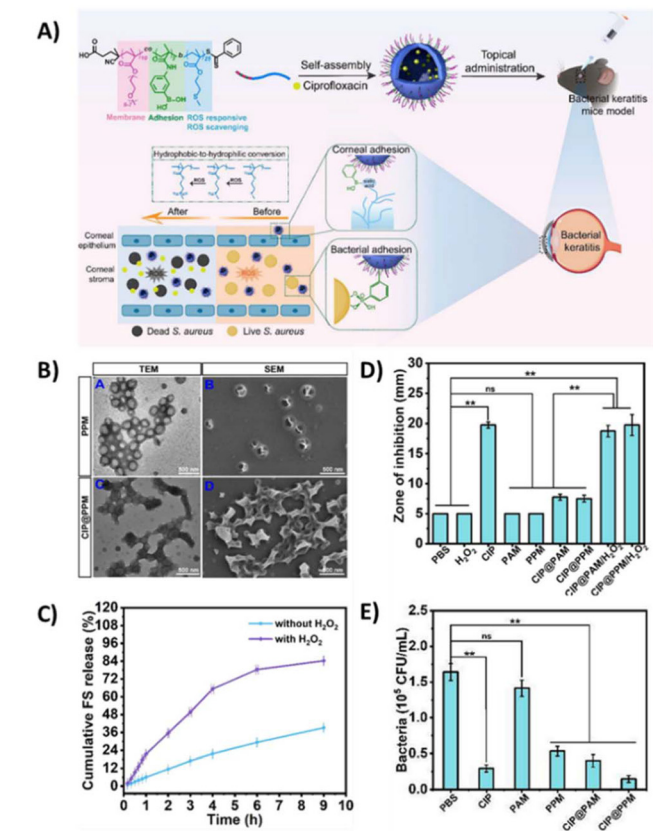


**Fig. 5** (A) Representative schematic of the study aimed to develop ciprofloxacin (CIP)-loaded P(PEGMA<sub>10</sub>-co-PBA<sub>2</sub>)-b-PMTEMA<sub>25</sub> polymersomes for the treatment of bacterial keratitis. (B) TEM and SEM micrographs of blank and CIP-loaded polymersomes. (C) Cumulative release of fluorescein sodium (FS) from polymersomes under stimulation of  $H_2O_2$ . (D) Antibacterial property of CIP loaded polymersomes against *S. aureus* with and without the ROS response, compared to blank polymersomes and control groups of PBS and  $H_2O_2$ . (E) Quantification of bacterial colonies formed of samples from mouse corneas, taken after the *in vivo* treatment of polymersomes (adapted with the permission from ref. 2. Copyright 2023, American Chemical Society.).

a network of zwitterionic polymersomes without an additional hydrogel matrix. Further advancing ocular drug delivery, Chen *et al.* developed ROS-responsive polymersomes from poly(poly-ethylene glycol methyl ethermethacrylate)-*co*-*N*-benzylacrylamide)-*block*-poly(2-methylthioethyl methacrylate) (P(PEGMA<sub>10</sub>-co-PBA<sub>2</sub>)-b-PMTEMA<sub>25</sub>) for the treatment of bacterial keratitis (BK), as seen in Fig. 5.<sup>2</sup> Ciprofloxacin (CIP)-loaded polymersomes (~247 nm) were produced using solvent switch method, achieving a loading capacity of 7.04%. The hydrophobic block of PMTEMA polymers was used for the ROS-responsive part of the polymersome, increasing membrane permeability upon  $H_2O_2$  exposure, which improved antibacterial effects against *S. aureus*.<sup>2</sup> Furthermore, the PBA block increased corneal retention as a mucoadhesive agent.<sup>2</sup> CIP-loaded polymersomes topical administered to wild-type C57BL/6j mice eyes twice a day for 7 days indicated superior antibacterial properties com-

pared to free CIP, suggesting their potential for topical ocular infection treatments.<sup>2</sup>

In our recent study, we developed sphingosine-grafted hyaluronan (HA-Sph) polymers with DS% from 15.45% to 23.34%, forming spherical polymersomes (~97.25–161.9 nm) with uniform size distributions.<sup>3</sup> These polymersomes selectively hindered tube formation and proliferation of HUVECs, thereby inhibit neovascularization in a dose-dependent manner, as shown in Fig. 6.<sup>3</sup> Notably, while free sphingosine exhibited cytotoxicity toward ARPE-19 cells and HUVECs, sphingosine-loaded polymersomes specifically suppressed HUVEC proliferation without harming ARPE-19 cells.<sup>3</sup> Cellular uptake study showed that rhodamine B (Rhod B)-loaded HA50Sph internalized by HUVECs *via* receptor mediated endocytosis (Fig. 6E). Additionally, the ability of these polymersomes to penetrate the ocular barriers was demonstrated by *ex vivo* whole porcine eye penetration study. When applied as topical eye drops, these polymersomes successfully reached the retina within 24 h (Fig. 6F).<sup>3</sup> This confirms the potential of polymersomes as effective topical drug delivery systems, particularly for targeting the posterior eye segment. The latest studies are important for demonstrating the effectiveness of polymersomes in overcoming ocular barriers, particularly when applied *via* the topical route.<sup>2,3</sup> Considering patient convenience and compliance, topical administration should be the preferred method. Currently, no nanocarrier system is available that can traverse ocular barriers and reach to the posterior segment of the eye with high drug loading. In this regard, polymersomes have the potential to overcome the challenges faced by current ocular drug delivery systems and may become the first choice for clinical applications in the future.

## 6. Future perspectives

Delivering drugs to the posterior segment of the eye is a highly challenging objective that demands specific strategies. The main obstacle in ocular drug delivery is the presence of barriers within the eye that hinder the passage of foreign compounds, thereby reducing the effectiveness of drug delivery. A number of ocular barriers such as the tear film, nasolacrimal drainage, cornea, conjunctiva, sclera, choroid, and blood-retinal barrier must be traversed by drug molecules and carriers in accordance with their chosen routes of administration.<sup>148,149</sup> Hence, formulations for drug delivery systems to the eyes must exhibit specific properties such as adhering to eye surfaces, targeted and prolonged drug release, ability to penetrate barriers, high drug bioavailability, minimal or no eye irritation, appropriate treatment frequency, and acceptable eye safety.<sup>150,151</sup>

Several types of nanomaterials have been investigated for ocular drug delivery, such as liposomes, niosomes, micelles, polymersomes, polymeric nanoparticles, and dendrimers.<sup>152</sup> Among them, liposomes and niosomes are widely accepted as ocular drug carriers.<sup>1,153</sup> Their physicochemical properties are well-known, and pharmacokinetics is evaluated



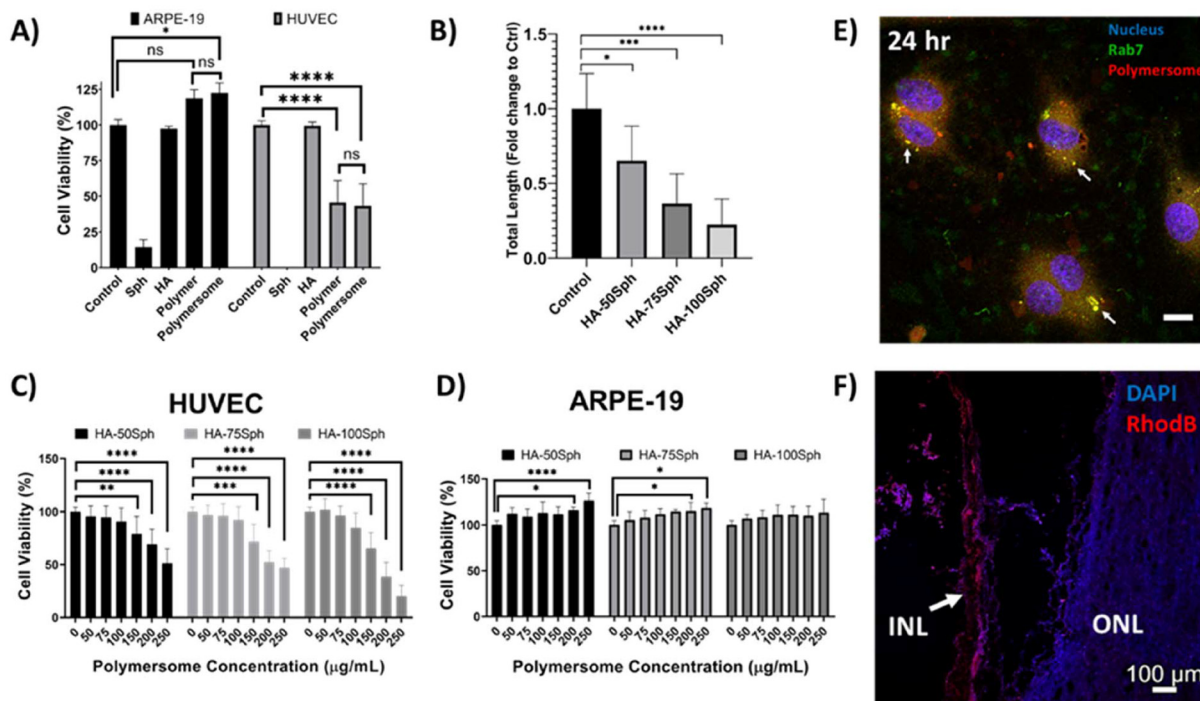


**Fig. 6** Cell viabilities of HUVEC and ARPE-19 cells against respective compounds. (A) Sph-grafted hyaluronan polymersomes ( $150 \mu\text{g mL}^{-1}$ ), polymer ( $150 \mu\text{g mL}^{-1}$ ), free Sph ( $55 \mu\text{M}$ ), and free hyaluronan. (B) Inhibition of tube formation with various polymersomes ( $150 \mu\text{g mL}^{-1}$ ). (C) and (D) Various concentrations of Sph-grafted hyaluronan polymersomes with degree of substitutions of 15.45%, 21.05%, 23.24% for HA-50Sph, HA-75Sph, and HA-100Sph, respectively. (E) Cellular uptake of Rhod B loaded polymersomes to HUVECs (scale bar:  $20 \mu\text{m}$ ). (F) Retina section of ex vivo whole porcine eye experiment after 24 h topical administration of Rhod B loaded polymersomes (scale bar:  $100 \mu\text{m}$ ) (INL: inner nuclear layer, ONL: outer nuclear layer) (reprinted under terms of the CC BY-NC license from ref. 3. Copyright 2024, Wiley).

considerably.<sup>154,155</sup> In particular, liposomes, supported by extensive research, hold a significant market share as drug delivery systems. After 2020, FDA approved 15 liposome-based

drug delivery systems, in which two of them (Visudyne®, which contains verteporfin for treatment of AMD and choroidal neovascularization and Tears Again®, which is a lubricant

**Table 2** FDA approved synthetic and natural polymers

	Polymer	Hydrophilicity	Approval of usage in ocular tissues	Ref.
Synthetic polymers	Poly(ethylene glycol) (PEG) <sup>a</sup>	Hydrophilic	Yes	89, 92, 125 and 168–170
	Poly(vinyl alcohol) (PVA) <sup>a</sup>	Hydrophilic	Yes	
	Poly(glycolide) (PGA)	Hydrophilic	Yes	
	Poly(glycolide- <i>co</i> -lactide) (PLGA) <sup>a</sup>	Hydrophobic	Yes	
	Poly(lactide) (PLA) <sup>a</sup>	Hydrophobic	Yes	
	Poly(methacrylates) (PMMA) <sup>a</sup>	Hydrophilic/hydrophobic	Yes	
	Poly(amidoamine) (PAMAM) <sup>a</sup>	Hydrophilic	No	
	Poly(caprolactone) (PCL) <sup>a</sup>	Hydrophobic	No	
	Poly(acrylic acid) (PAA) <sup>a</sup>	Hydrophilic/hydrophobic	Yes	
	Poly(orthoester) (POE)	Hydrophobic	No	
Natural polymers	Hyaluronan <sup>a</sup>	Hydrophilic	Yes	3, 62, 72, 73, 168 and 171–173
	Chitosan <sup>a</sup>	Hydrophilic	Yes	
	Alginate <sup>a</sup>	Hydrophilic	No	
	Gelatin <sup>a</sup>	Hydrophilic	Yes	
	Collagen	Amphiphilic	Yes	
	Cellulose	Hydrophilic	Yes	
	Carboxymethyl cellulose (CMC) <sup>a</sup>	Hydrophilic	Yes	
	Guar gum	Hydrophilic	Yes	
	Dextran <sup>a</sup>	Hydrophilic	Yes	
	Pullulan <sup>a</sup>	Hydrophilic	Yes	

<sup>a</sup> Indicates the polymers utilized in polymersomes preparation.

spray for dry eye treatment) are approved for ocular diseases.<sup>156</sup> However, liposomal systems have difficulties in storage, short half-lives, low encapsulation efficiency for hydrophilic drugs and they can cause cloudiness in the vitreous and obstruct the vision.<sup>156,157</sup> Moreover, liposomes have low mucoadhesive properties and often necessitates coating of mucoadhesive polymers, *e.g.* hyaluronan or chitosan, to improve preocular retention and prolonged drug delivery.<sup>157,158</sup>

Polymersomes have ideal properties for ocular drug delivery including traversing ocular barriers, mechanical stability, ocular retention capability, simultaneous encapsulation of hydrophilic and hydrophobic drugs, and stimuli responsive controlled release. Aibani *et al.* conducted a recent study on polymersomes, comparing them with liposomes in terms of size, stability, encapsulation efficiency, drug release, cellular uptake, and toxicity.<sup>159</sup> This comparative study of polymersomes with their strongest alternative, liposomes, demonstrated their higher storage stability at 25 °C for 8 weeks.<sup>159</sup> When compared with polymeric micelles, for instance DOX-loaded PEG-PDLLA polymeric micelles, polymersomes exhibit higher drug encapsulation efficiency and better *in vitro* stability.<sup>160</sup> Although there are many encouraging studies on polymersomes as drug carriers, the majority of them are still in the preclinical stage. The limited availability of amphiphilic copolymers in the market might potentially be slowing down the commercialization of polymersomes.<sup>161</sup> Despite this limitation, a number of polymeric micelles such as SP1049C (Pluronic F127-Pluronic L61), Genexol-PM (mPEG-PDLLA), and Nanoxel-PM (mPEG-PDLLA) have been approved by the FDA (Table 2) or are in clinical trials.<sup>161–164</sup> The growing research on design and application of amphiphilic polymers and polymersomes indicates a potential expansion in the field.<sup>125,165–167</sup>

Previously, Mattoori and Leroux asked about which clinical applications necessitates tougher membranes than liposomal ones, by addressing the thicker and tougher membrane of polymersomes.<sup>64</sup> Our answer to this question is ocular drug delivery applications, which necessitates tougher membranes that could withstand dynamic ocular barriers such as tear, while the membrane should be flexible enough to squeeze and pass through the static ocular barriers such as blood-retinal barrier. Needless to say, polymersomes, combining tough yet flexible membranes with other advantageous properties, hold great potential to be applied as a delivery system for the ocular tissues. Future research should focus on tailoring polymersome membranes to balance toughness and flexibility specifically for the ocular environment, as well as developing scalable manufacturing approaches to accelerate clinical translation.

## 7. Conclusions

Polymersomes, self-assembled from amphiphilic copolymers, represent a highly versatile and promising platform for drug delivery applications. While their potential has been widely explored in cancer therapy, their unique chemical and physical

characteristics also position them as strong candidates for ocular drug delivery. Compared to conventional vesicular systems such as liposomes and niosomes, polymersomes offer superior control over size, membrane properties, mucoadhesive properties, drug encapsulation, and release profiles, enabling them to overcome the multiple barriers of the eye. Their ability to encapsulate both hydrophilic and hydrophobic compounds, combined with mechanical robustness and stimuli-responsiveness, makes them particularly suitable for reaching the posterior segment of the eye, even with topical administrations. Additionally, they can be biodegradable and offer a safer alternative which does not blur the vision after administration. Although these benefits are noteworthy, it is important to address possible toxicity of polymersomes and their degradation by-products. Further investigations using polymersomes made from FDA-approved polymers may help address this limitation.

Despite the encouraging properties demonstrated at the preclinical level, the translation of polymersomes into clinical ophthalmology still faces several challenges, including polymer bioavailability, scalability, regulatory approval, and comprehensive safety profiling. Nonetheless, the increasing understanding of polymersome behaviour within ocular tissues, combined with advances in polymer science and nanomedicine, is expected to drive further development. With their tunable design and capacity to meet the complex requirements of ocular delivery, polymersomes offer a compelling and adaptable solution for future ophthalmic therapeutics.

## Author contributions

A. A. Y.: conceptualization, investigation, validation, visualization, writing – original draft, writing – review & editing, project administration. P. M. S.: writing – original draft, validation, funding acquisition. S. C.: conceptualization, validation, writing – review & editing, funding acquisition, project administration, supervision.

## Data availability

No primary research results, software or code have been included, and no new data were generated or analysed as part of this review.

## Conflicts of interest

There are no conflicts to declare.

## Acknowledgements

The authors would like to acknowledge The Scientific and Technological Research Council of Türkiye (TUBITAK) for the funding support for PhD scholarship through BİDEB-2244



program (grant number: 118C146) and for the funding support for researcher co-circulation through BIDEB-2236 program (grant number: 120C060). AAY would like to thank the Sabancı University Faculty of Engineering and Natural Sciences for the support as postdoctoral scholarship.

## References

- 1 S. Durak, M. Esmaeili Rad, A. Alp Yetisgin, H. Eda Sutova, O. Kutlu, S. Cetinel and A. Zarrabi, *Nanomaterials*, 2020, **10**, 1191.
- 2 Q. Chen, X. Han, L. Liu, Y. Duan, Y. Chen, L. Shi, Q. Lin and L. Shen, *Biomacromolecules*, 2023, **24**, 5230–5244.
- 3 A. A. Yetisgin, S. Durak, O. Kutlu and S. Cetinel, *Macromol. Biosci.*, 2024, **24**, e2300531.
- 4 L. Bonilla, M. Espina, P. Severino, A. Cano, M. Ettcheto, A. Camins, M. L. Garcia, E. B. Souto and E. Sanchez-Lopez, *Pharmaceutics*, 2021, **14**, 90.
- 5 Y. Wang and C. Wang, *Pharmaceutics*, 2022, **14**, 1150.
- 6 R. A. Alshaikh, C. Waeber and K. B. Ryan, *Adv. Drug Delivery Rev.*, 2022, **187**, 114342.
- 7 E. Himawan, P. Ekstrom, M. Buzgo, P. Gaillard, E. Stefansson, V. Marigo, T. Loftsson and F. Paquet-Durand, *Drug Discovery Today*, 2019, **24**, 1637–1643.
- 8 E. M. Karasavvidou, P. Tranos and G. D. Panos, *Drug Des., Dev. Ther.*, 2022, **16**, 2659–2680.
- 9 H. M. Kim and S. J. Woo, *Pharmaceutics*, 2021, **13**, 108.
- 10 Y. Weng, J. Liu, S. Jin, W. Guo, X. Liang and Z. Hu, *Acta Pharm. Sin. B*, 2017, **7**, 281–291.
- 11 C. G. Zhang, R. L. Zhang, Y. Zhu, W. Wei, Y. Gu and X. Y. Liu, *Mater. Lett.*, 2016, **164**, 15–18.
- 12 E. Aydinlioglu, M. Abdelghani, G. Le Fer, J. C. M. van Hest, O. Sandre and S. Lecommandoux, *Macromol. Chem. Phys.*, 2023, **224**, 2200306.
- 13 S. Iqbal, M. Blenner, A. Alexander-Bryant and J. Larsen, *Biomacromolecules*, 2020, **21**, 1327–1350.
- 14 A. Subrizi, E. M. Del Amo, V. Korzhikov-Vlakh, T. Tennikova, M. Ruponen and A. Urtti, *Drug Discovery Today*, 2019, **24**, 1446–1457.
- 15 S. Gorantla, V. K. Rapalli, T. Waghule, P. P. Singh, S. K. Dubey, R. N. Saha and G. Singhvi, *RSC Adv.*, 2020, **10**, 27835–27855.
- 16 S. Ahmed, M. M. Amin and S. Sayed, *AAPS PharmSciTech*, 2023, **24**, 66.
- 17 K. Y. Wu, M. Joly-Chevrier, D. Akbar and S. D. Tran, *Pharmaceutics*, 2023, **15**, 1094.
- 18 D. H. Geroski and H. F. Edelhauser, *Invest. Ophthalmol. Visual Sci.*, 2000, **41**, 961–964.
- 19 C. Amador, R. Shah, S. Ghiam, A. A. Kramerov and A. V. Ljubimov, *Curr. Gene Ther.*, 2022, **22**, 104–131.
- 20 P. Bhatt, S. Kelly and V. Sutariya, *Ther. Delivery*, 2019, **10**, 737–747.
- 21 V. Junnuthula, A. Sadeghi Boroujeni, S. Cao, S. Tavakoli, R. Ridolfo, E. Toropainen, M. Ruponen, J. C. M. van Hest and A. Urtti, *Pharmaceutics*, 2021, **13**, 445.
- 22 R. Suri, S. Beg and K. Kohli, *J. Drug Delivery Sci. Technol.*, 2020, **55**, 101389.
- 23 M. Singh, S. Bharadwaj, K. E. Lee and S. G. Kang, *J. Controlled Release*, 2020, **328**, 895–916.
- 24 R. Varela-Fernandez, V. Diaz-Tome, A. Luaces-Rodriguez, A. Conde-Penedo, X. Garcia-Otero, A. Lizardo-Alvarez, A. Fernandez-Ferreiro and F. J. Otero-Espinar, *Pharmaceutics*, 2020, **12**, 269.
- 25 E. A. Mun, P. W. Morrison, A. C. Williams and V. V. Khutoryanskiy, *Mol. Pharm.*, 2014, **11**, 3556–3564.
- 26 M. Fucito, M. Spedicato, S. Felletti, A. C. Yu, M. Busin, L. Pasti, F. A. Franchina, A. Cavazzini, C. De Luca and M. Catani, *ACS Meas. Sci. Au*, 2024, **4**, 247–259.
- 27 S. Lin, C. Ge, D. Wang, Q. Xie, B. Wu, J. Wang, K. Nan, Q. Zheng and W. Chen, *ACS Appl. Mater. Interfaces*, 2019, **11**, 39603–39612.
- 28 T. J. Shah, M. D. Conway and G. A. Peyman, *Clin. Ophthalmol.*, 2018, **12**, 2223–2235.
- 29 M. C. Callegan, M. S. Gilmore, M. Gregory, R. T. Ramadan, B. J. Wiskur, A. L. Moyer, J. J. Hunt and B. D. Novosad, *Prog. Retinal Eye Res.*, 2007, **26**, 189–203.
- 30 D. Y. Park, J. Lee, J. Kim, K. Kim, S. Hong, S. Han, Y. Kubota, H. G. Augustin, L. Ding, J. W. Kim, H. Kim, Y. He, R. H. Adams and G. Y. Koh, *Nat. Commun.*, 2017, **8**, 15296.
- 31 S. Li, L. Chen and Y. Fu, *J. Nanobiotechnol.*, 2023, **21**, 232.
- 32 P. Agarwal and I. D. Rupenthal, *Adv. Drug Delivery Rev.*, 2023, **198**, 114867.
- 33 D. Huang, Y. S. Chen and I. D. Rupenthal, *Adv. Drug Delivery Rev.*, 2018, **126**, 96–112.
- 34 M. B. Ozturk, M. Popa, D. M. Rata, A. N. Cadinoiu, F. Parfait, C. Delaite, L. I. Atanase, C. Solcan and O. M. Daraba, *Int. J. Mol. Sci.*, 2022, **23**, 9382.
- 35 M. Gautam, R. Gupta, P. Singh, V. Verma, S. Verma, P. Mittal, S. Karkhur, A. Sampath, R. R. Mohan and B. Sharma, *J. Ocul. Pharmacol. Ther.*, 2023, **39**, 102–116.
- 36 E. Mann, J. A. Kammer, G. Sawhney, J. An, E. C. Werts, V. Vera, M. Rivas, H. Lai, S. Sonparote and E. R. Craven, *Drugs*, 2025, **85**, 397–414.
- 37 C. H. Tsai, L. N. Hoang, C. C. Lin, L. C. Pan, C. L. Wu, I. C. Lin, P. Y. Wang and C. L. Tseng, *Pharmaceutics*, 2022, **14**, 1253.
- 38 S. Galindo, A. de la Mata, M. Lopez-Paniagua, J. M. Herreras, I. Perez, M. Calonge and T. Nieto-Miguel, *Stem Cell Res. Ther.*, 2021, **12**, 60.
- 39 L. A. Lam, S. Mehta, E. M. Lad, G. G. Emerson, J. M. Jumper, C. C. Awh and S. Task, *Force on Intravitreal Injection Supplemental*, *J. Vitreoretin. Dis.*, 2021, **5**, 438–447.
- 40 A. Than, C. Liu, H. Chang, P. K. Duong, C. M. G. Cheung, C. Xu, X. Wang and P. Chen, *Nat. Commun.*, 2018, **9**, 4433.
- 41 N. A. Grimm, S. Fahimi, F. Kuck, P. Take, P. Lauermann, A. Nguyen-Hoehl, H. Hoerauf, N. Feltgen and S. Bemme, *Graefes Arch. Clin. Exp. Ophthalmol.*, 2023, **261**, 2421–2429.
- 42 S. Naik, A. B. Shreya, R. Raychaudhuri, A. Pandey, S. A. Lewis, M. Hazarika, S. V. Bhandary, B. S. S. Rao and S. Mutualik, *Life Sci.*, 2021, **264**, 118712.



43 J. S. Lee, J. Y. Kim, C. Jung and S. J. Woo, *Prog. Retinal Eye Res.*, 2020, **78**, 100848.

44 K. Y. Wu, J. K. Fujioka, T. Gholamian, M. Zaharia and S. D. Tran, *Pharmaceutics*, 2023, **16**, 1241.

45 B. Grassiri, Y. Zambito and A. Bernkop-Schnurch, *Adv. Colloid Interface Sci.*, 2021, **288**, 102342.

46 J. Kour, N. Kumari and B. Sapra, *Asian J. Pharm. Sci.*, 2021, **16**, 175–191.

47 R. V. Moiseev, P. W. J. Morrison, F. Steele and V. V. Khutoryanskiy, *Pharmaceutics*, 2019, **11**, 321.

48 C. Liu, L. Tai, W. Zhang, G. Wei, W. Pan and W. Lu, *Mol. Pharm.*, 2014, **11**, 1218–1227.

49 P. L. Destruel, N. Zeng, J. Seguin, S. Douat, F. Rosa, F. Brignole-Baudouin, S. Dufay, A. Dufay-Wojcicki, M. Maury, N. Mignet and V. Boudy, *Int. J. Pharm.*, 2020, **574**, 118734.

50 S. H. S. Boddu, D. Acharya, V. Hala, H. Jani, S. Pande, C. Patel, M. Shahwan, R. Jwala and K. M. Ranch, *ACS Omega*, 2023, **8**, 35470–35498.

51 R. S. Bhatta, H. Chandasana, Y. S. Chhonker, C. Rathi, D. Kumar, K. Mitra and P. K. Shukla, *Int. J. Pharm.*, 2012, **432**, 105–112.

52 R. Yan, L. Xu, Q. Wang, Z. Wu, H. Zhang and L. Gan, *Mol. Pharm.*, 2021, **18**, 4290–4298.

53 M. Kabiri, S. H. Kamal, S. V. Pawar, P. R. Roy, M. Derakhshandeh, U. Kumar, S. G. Hatzikiriakos, S. Hossain and V. G. Yadav, *Drug Delivery Transl. Res.*, 2018, **8**, 484–495.

54 F. Ullrich, C. Bergeles, J. Pokki, O. Ergeneman, S. Erni, G. Chatzipirpiridis, S. Pane, C. Framme and B. J. Nelson, *Invest. Ophthalmol. Visual Sci.*, 2013, **54**, 2853–2863.

55 H. Han, S. Li, M. Xu, Y. Zhong, W. Fan, J. Xu, T. Zhou, J. Ji, J. Ye and K. Yao, *Adv. Drug Delivery Rev.*, 2023, **196**, 114770.

56 K. Tahara, K. Karasawa, R. Onodera and H. Takeuchi, *Asian J. Pharm. Sci.*, 2017, **12**, 394–399.

57 L. Guidi, M. G. Cascone and E. Rosellini, *Helyon*, 2024, **10**, e26616.

58 N. M. Nguyen Le, S. Zsak, B. Le-Vinh, J. D. Friedl, G. Kali, P. Knoll, H. W. Seitter, A. Koschak and A. Bernkop-Schnurch, *ACS Appl. Mater. Interfaces*, 2022, **14**, 44981–44991.

59 A. J. Bailey, *Eye*, 1987, **1**(Pt 2), 175–183.

60 C. H. Tsai, P. Y. Wang, I. C. Lin, H. Huang, G. S. Liu and C. L. Tseng, *Int. J. Mol. Sci.*, 2018, **19**, 2830.

61 S. Kim, J. Fan, C. S. Lee and M. Lee, *ACS Appl. Bio Mater.*, 2020, **3**, 2334–2343.

62 P. M. Sivakumar, A. A. Yetisgin, S. B. Sahin, E. Demir and S. Cetinel, *Carbohydr. Polym.*, 2022, **283**, 119142.

63 D. E. Discher and A. Eisenberg, *Science*, 2002, **297**, 967–973.

64 S. Mattoori and J.-C. Leroux, *Mater. Horiz.*, 2020, **7**, 1297–1309.

65 J. C. van Hest, D. A. Delnoye, M. W. Baars, M. H. van Genderen and E. W. Meijer, *Science*, 1995, **268**, 1592–1595.

66 L. Zhang and A. Eisenberg, *Science*, 1995, **268**, 1728–1731.

67 B. M. Discher, Y. Y. Won, D. S. Ege, J. C. Lee, F. S. Bates, D. E. Discher and D. A. Hammer, *Science*, 1999, **284**, 1143–1146.

68 Y. Hu and L. Qiu, *Methods Mol. Biol.*, 2019, **2000**, 247–265.

69 A. K. Sharma, P. Prasher, A. A. Aljabali, V. Mishra, H. Gandhi, S. Kumar, S. Mutualik, D. K. Chellappan, M. M. Tambuwala, K. Dua and D. N. Kapoor, *Drug Delivery Transl. Res.*, 2020, **10**, 1171–1190.

70 N. P. Iakimov, M. A. Zotkin, E. A. Dets, S. S. Abramchuk, A. M. Arutyunian, I. D. Grozdova and N. S. Melik-Nubarov, *Colloid Polym. Sci.*, 2021, **299**, 1543–1555.

71 K. Kuperkar, D. Patel, L. I. Atanase and P. Bahadur, *Polymers*, 2022, **14**, 4702.

72 Z. Wu, H. Li, X. Zhao, F. Ye and G. Zhao, *Carbohydr. Polym.*, 2022, **284**, 119182.

73 T. Nishimura, S. Fujii, K. Sakurai, Y. Sasaki and K. Akiyoshi, *Macromolecules*, 2021, **54**, 7003–7009.

74 Y. Sakamoto and T. Nishimura, *Polym. Chem.*, 2022, **13**, 6343–6360.

75 M. Antonietti and S. Förster, *Adv. Mater.*, 2003, **15**, 1323–1333.

76 K. Kita-Tokarczyk, J. Grumelard, T. Haefele and W. Meier, *Polymer*, 2005, **46**, 3540–3563.

77 C. Lin, K. Siddharth and J. Perez-Mercader, *RSC Adv.*, 2025, **15**, 4693–4700.

78 J. M. Zhang, J. H. Jiang, S. Lin, E. J. Cornel, C. Li and J. Z. Du, *Chin. J. Chem.*, 2022, **40**, 1842–1855.

79 Q. C. Zhang, R. M. Zeng, Y. X. Zhang, Y. Chen, L. Zhang and J. B. Tan, *Macromolecules*, 2020, **53**, 8982–8991.

80 J. Lefley, C. Waldron and C. R. Becer, *Polym. Chem.*, 2020, **11**, 7124–7136.

81 A. Ianiro, H. Wu, M. M. J. van Rijt, M. P. Vena, A. D. A. Keizer, A. C. C. Esteves, R. Tuinier, H. Friedrich, N. Sommerdijk and J. P. Patterson, *Nat. Chem.*, 2019, **11**, 320–328.

82 S. Varlas, J. C. Foster, P. G. Georgiou, R. Keogh, J. T. Husband, D. S. Williams and R. K. O'Reilly, *Nanoscale*, 2019, **11**, 12643–12654.

83 P. V. Pawar, S. V. Gohil, J. P. Jain and N. Kumar, *Polym. Chem.*, 2013, **4**, 3160–3176.

84 H. Xu, W. Cui, Z. Zong, Y. Tan, C. Xu, J. Cao, T. Lai, Q. Tang, Z. Wang, X. Sui and C. Wang, *Drug Delivery*, 2022, **29**, 2414–2427.

85 P. Walvekar, R. Gannimani, M. Salih, S. Makhathini, C. Mocktar and T. Govender, *Colloids Surf. B*, 2019, **182**, 110388.

86 A. C. Greene, I. M. Henderson, A. Gomez, W. F. Paxton, V. VanDelinder and G. D. Bachand, *PLoS One*, 2016, **11**, e0158729.

87 C. D. Tan, M. Scholler and E. K. Ehmoser, *Gels*, 2025, **11**, 29.

88 M. Dionzou, A. Morere, C. Roux, B. Lonetti, J. D. Marty, C. Mingotaud, P. Joseph, D. Goudouneche, B. Payre, M. Leonetti and A. F. Mingotaud, *Soft Matter*, 2016, **12**, 2166–2176.

89 U. C. Oz, Z. B. Bolat, U. U. Ozkose, S. Gulyuz, B. Kucukturkmen, M. P. Khalily, S. Ozcubukcu, O. Yilmaz,



D. Telci, G. Esen dagli, F. Sahin and A. Bozkir, *Mater. Sci. Eng., C*, 2021, **123**, 111929.

90 C. K. Wong, A. F. Mason, M. H. Stenzel and P. Thordarson, *Nat. Commun.*, 2017, **8**, 1240.

91 I. Meerovich and A. K. Dash, in *Materials for Biomedical Engineering*, 2019, pp. 269–309, DOI: [10.1016/b978-0-12-818433-2.00008.x](https://doi.org/10.1016/b978-0-12-818433-2.00008.x).

92 V. Singh, S. Md, N. A. Alhakamy and P. Kesharwani, *Eur. Polym. J.*, 2022, **162**, 110883.

93 V. Balasubramanian, B. Herranz-Blanco, P. V. Almeida, J. Hirvonen and H. A. Santos, *Prog. Polym. Sci.*, 2016, **60**, 51–85.

94 S. Allen, O. Osorio, Y. G. Liu and E. Scott, *J. Controlled Release*, 2017, **262**, 91–103.

95 M. Alibolandi, K. Abnous, F. Hadizadeh, S. M. Taghdisi, F. Alabdollah, M. Mohammadi, H. Nassirli and M. Ramezani, *J. Controlled Release*, 2016, **241**, 45–56.

96 E. Rideau, R. Dimova, P. Schwille, F. R. Wurm and K. Landfester, *Chem. Soc. Rev.*, 2018, **47**, 8572–8610.

97 R. Kotha, D. D. Kara, R. Roychowdhury, K. Tanvi and M. Rathnanand, *Adv. Pharm. Bull.*, 2023, **13**, 218–232.

98 N. Dan, in *Design and Development of New Nanocarriers*, ed. A. M. Grumezescu, William Andrew Publishing, 2018, pp. 1–55, DOI: [10.1016/b978-0-12-813627-0.00001-6](https://doi.org/10.1016/b978-0-12-813627-0.00001-6).

99 C. K. Wong, R. Y. Lai and M. H. Stenzel, *Nat. Commun.*, 2023, **14**, 6237.

100 A. Martin, P. Lalanne, A. Weber-Vax, A. Mutschler and S. Lecommandoux, *Int. J. Pharm.*, 2023, **642**, 123157.

101 T. Batista Napotnik, G. Bello, E. K. Sinner and D. Miklavcic, *J. Membr. Biol.*, 2017, **250**, 441–453.

102 M. Hasannia, A. Aliabadi, K. Abnous, S. M. Taghdisi, M. Ramezani and M. Alibolandi, *J. Controlled Release*, 2022, **341**, 95–117.

103 H. R. Marsden, L. Gabrielli and A. Kros, *Polym. Chem.*, 2010, **1**, 1512–1518.

104 C. Sanson, C. Schatz, J. F. Le Meins, A. Brulet, A. Soum and S. Lecommandoux, *Langmuir*, 2010, **26**, 2751–2760.

105 Y. J. Men, F. Peng, Y. F. Tu, J. C. M. van Hest and D. A. Wilson, *Polym. Chem.*, 2016, **7**, 3977–3982.

106 S. Yorulmaz Avsar, M. Kyropoulou, S. Di Leone, C. A. Schoenenberger, W. P. Meier and C. G. Palivan, *Front. Chem.*, 2018, **6**, 645.

107 R. Y. P. da Silva, L. C. G. da Silva, M. F. C. S. Ricardo and Á. A. N. de Lima, in *Pharmaceutical Nanobiotechnology for Targeted Therapy*, ed. H. Barabadi, E. Mostafavi and M. Saravanan, Springer International Publishing, Cham, 2022, ch. 14, pp. 399–427, DOI: [10.1007/978-3-031-12658-1\\_14](https://doi.org/10.1007/978-3-031-12658-1_14).

108 M. S. Muthwill, P. Kong, I. A. Dinu, D. Necula, C. John and C. G. Palivan, *Macromol. Biosci.*, 2022, **22**, e2200270.

109 P. Pallavi, K. Harini, P. Gowtham, K. Girigoswami and A. Girigoswami, *Chemistry*, 2022, **4**, 1028–1043.

110 K. K. Upadhyay, A. N. Bhatt, E. Castro, A. K. Mishra, K. Chuttani, B. S. Dwarakanath, C. Schatz, J. F. Le Meins, A. Misra and S. Lecommandoux, *Macromol. Biosci.*, 2010, **10**, 503–512.

111 S. Haas, N. Hain, M. Raoufi, S. Handschuh-Wang, T. Wang, X. Jiang and H. Schonherr, *Biomacromolecules*, 2015, **16**, 832–841.

112 M. Shahriari, S. M. Taghdisi, K. Abnous, M. Ramezani and M. Alibolandi, *J. Controlled Release*, 2021, **335**, 369–388.

113 F. Ahmed, R. I. Pakunlu, G. Srinivas, A. Brannan, F. Bates, M. L. Klein, T. Minko and D. E. Discher, *Mol. Pharm.*, 2006, **3**, 340–350.

114 M. Kim, D. Kim, Y. Jang, H. Han, S. Lee, H. Moon, J. Kim and H. Kim, *Int. J. Mol. Sci.*, 2023, **24**, 1194.

115 Q. Hu, F. Zhang, Y. Wei, J. Liu, Y. Nie, J. Xie, L. Yang, R. Luo, B. Shen and Y. Wang, *Biomacromolecules*, 2023, **24**, 3532–3544.

116 B. Mamnoon, A. S. Moses, S. Sundaram, C. J. Raitmayr, T. Morgan, M. K. Baldwin, L. Myatt, O. Taratula and O. R. Taratula, *Small*, 2024, **20**, e2302969.

117 E. Scarpa, A. A. Janeczek, A. Hailes, M. C. de Andres, A. De Grazia, R. O. Oreffo, T. A. Newman and N. D. Evans, *Nanomedicine*, 2018, **14**, 1267–1277.

118 Y. Zhang, K. Wu, H. Sun, J. Zhang, J. Yuan and Z. Zhong, *ACS Appl. Mater. Interfaces*, 2018, **10**, 1597–1604.

119 F. Karandish, J. Froberg, P. Borowicz, J. C. Wilkinson, Y. Choi and S. Mallik, *Colloids Surf., B*, 2018, **163**, 225–235.

120 J. Leong, J. Y. Teo, V. K. Aakalu, Y. Y. Yang and H. Kong, *Adv. Healthcare Mater.*, 2018, **7**, e1701276.

121 J. F. Scheerstra, A. C. Wauters, J. Tel, L. K. E. A. Abdelmohsen and J. C. M. van Hest, *Mater. Today Adv.*, 2022, **13**, 100203.

122 T. Anajafi and S. Mallik, *Ther. Delivery*, 2015, **6**, 521–534.

123 F. H. Sobotta, M. T. Kuchenbrod, F. V. Gruschwitz, G. Festag, P. Bellstedt, S. Hoeppener and J. C. Brendel, *Angew. Chem., Int. Ed.*, 2021, **60**, 24716–24723.

124 F. Araste, A. Aliabadi, K. Abnous, S. M. Taghdisi, M. Ramezani and M. Alibolandi, *J. Controlled Release*, 2021, **330**, 502–528.

125 M. G. Gouveia, J. P. Wesseler, J. Ramaekers, C. Weder, P. B. V. Scholten and N. Bruns, *Chem. Soc. Rev.*, 2023, **52**, 728–778.

126 M. Borhaninia, M. Zahiri, K. Abnous, S. M. Taghdisi, M. Ramezani and M. Alibolandi, *Int. J. Biol. Macromol.*, 2023, **248**, 125882.

127 C. Ferrero, M. Casas and I. Caraballo, *Pharmaceutics*, 2022, **14**, 1724.

128 H. J. Lee, A. Ponta and Y. Bae, *Ther. Delivery*, 2010, **1**, 803–817.

129 T. Zavar, M. Babaei, K. Abnous, S. M. Taghdisi, S. Nekooei, M. Ramezani and M. Alibolandi, *Int. J. Pharm.*, 2020, **578**, 119091.

130 N. A. D'Angelo, M. C. C. Câmara, M. A. Noronha, D. Grotto, M. Chorilli, F. R. Lourenço, C. D. Rangel-Yagui and A. M. Lopes, *J. Mol. Liq.*, 2022, **349**, 118166.

131 W. C. Huang, Y. C. Chen, Y. H. Hsu, W. Y. Hsieh and H. C. Chiu, *Colloids Surf., B*, 2015, **128**, 67–76.



132 C. Y. Yoo, J. S. Seong and S. N. Park, *Colloids Surf., B*, 2016, **144**, 99–107.

133 A. K. Tewari, S. C. Upadhyay, M. Kumar, K. Pathak, D. Kaushik, R. Verma, S. Bhatt, E. E. S. Massoud, M. H. Rahman and S. Cavalu, *Polymers*, 2022, **14**, 3545.

134 Y. Zhu, S. Cao, M. Huo, J. C. M. van Hest and H. Che, *Chem. Sci.*, 2023, **14**, 7411–7437.

135 S. Wang, Z. Li, L. Zhao, Y. Lin and H. Che, *Biomacromolecules*, 2025, **26**, 1251–1259.

136 B. Mamnoon, A. P. M. Souza, T. Korzun, M. K. Baldwin, K. S. Sharma, O. Taratula, Y. T. Goo, P. Singh, V. Grigoriev, A. Lakhanpal and O. R. Taratula, *Small Sci.*, 2025, 2400361.

137 M. Curcio, G. Cirillo, O. Vittorio, U. G. Spizzirri, F. Iemma and N. Picci, *Eur. Polym. J.*, 2015, **67**, 304–313.

138 J. Torres, N. Dhas, M. Longhi and M. C. Garcia, *Front. Pharmacol.*, 2020, **11**, 593197.

139 Y. C. Chen, C. F. Chiang, L. F. Chen, P. C. Liang, W. Y. Hsieh and W. L. Lin, *Biomaterials*, 2014, **35**, 4066–4081.

140 A. Joseph, C. Contini, D. Cecchin, S. Nyberg, L. Ruiz-Perez, J. Gaitzsch, G. Fullstone, X. Tian, J. Azizi, J. Preston, G. Volpe and G. Battaglia, *Sci. Adv.*, 2017, **3**, e1700362.

141 J. Shao, S. Cao, D. S. Williams, L. Abdelmohsen and J. C. M. van Hest, *Angew. Chem., Int. Ed.*, 2020, **59**, 16918–16925.

142 R. Ridolfo, S. Tavakoli, V. Junnuthula, D. S. Williams, A. Urtti and J. C. M. van Hest, *Biomacromolecules*, 2021, **22**, 126–133.

143 V. Junnuthula, A. S. Boroujeni, S. Cao, S. Tavakoli, R. Ridolfo, E. Toropainen, M. Ruponen, J. C. M. van Hest and A. Urtti, *Pharmaceutics*, 2021, **13**, 445.

144 A. Sadeghi, M. Ruponen, J. Puranen, S. Cao, R. Ridolfo, S. Tavakoli, E. Toropainen, T. Lajunen, V. P. Ranta, J. van Hest and A. Urtti, *Int. J. Pharm.*, 2022, **621**, 121800.

145 M. Sen, M. Al-Amin, E. Kickova, A. Sadeghi, J. Puranen, A. Urtti, P. Caliceti, S. Salmaso, B. Arango-Gonzalez and M. Ueffing, *J. Controlled Release*, 2021, **339**, 307–320.

146 D. C. S. de Oliveira, C. F. de Freitas, I. R. Calori, R. S. Goncalves, C. Cardinali, L. C. Malacarne, M. I. Ravanelli, H. P. M. de Oliveira, A. C. Tedesco, W. Caetano, N. Hioka and A. L. Tessaro, *J. Photochem. Photobiol., B*, 2020, **212**, 112039.

147 S. L. Banerjee, S. Samanta, S. Sarkar and N. K. Singha, *J. Mater. Chem. B*, 2020, **8**, 226–243.

148 X. Fan, K. Jiang, F. Geng, W. Lu and G. Wei, *Adv. Drug Delivery Rev.*, 2023, **197**, 114864.

149 X. Wang, F. Luan, H. Yue, C. Song, S. Wang, J. Feng, X. Zhang, W. Yang, Y. Li, W. Wei and Y. Tao, *Adv. Drug Delivery Rev.*, 2023, **200**, 115006.

150 C. Wang and Y. Pang, *Adv. Drug Delivery Rev.*, 2023, **194**, 114721.

151 A. A. Yetisgin, S. Cetinel, M. Zuvin, A. Kosar and O. Kutlu, *Molecules*, 2020, **25**, 2193.

152 I. Seah, X. Zhao, Q. Lin, Z. Liu, S. Z. Z. Su, Y. S. Yuen, W. Hunziker, G. Lingam, X. J. Loh and X. Su, *Eye*, 2020, **34**, 1341–1356.

153 N. Tasharrofi, M. Nourozi and A. Marzban, *J. Drug Delivery Sci. Technol.*, 2022, **67**, 103045.

154 S. N. Sanap, A. C. Bisen, A. Mishra, A. Biswas, S. Agrawal, K. S. Yadav, A. Krishna, S. Chopra, M. N. Mugale and R. S. Bhatta, *J. Drug Delivery Sci. Technol.*, 2022, **74**, 103517.

155 S. Lai, Y. Wei, Q. Wu, K. Zhou, T. Liu, Y. Zhang, N. Jiang, W. Xiao, J. Chen, Q. Liu and Y. Yu, *J. Nanobiotechnol.*, 2019, **17**, 64.

156 B. R. Giri, D. Jakka, M. A. Sandoval, V. R. Kulkarni and Q. Bao, *Pharmaceutics*, 2024, **16**, 1325.

157 E. Batur, S. Ozdemir, M. E. Durgun and Y. Ozsoy, *Pharmaceutics*, 2024, **17**, 511.

158 Y. Wang, Y. H. Hu, J. Y. An, H. Zhang, X. Liu, X. R. Li, Z. Z. Zhang and X. M. Zhang, *Adv. Funct. Mater.*, 2024, **34**, 2403142.

159 N. Aibani, T. N. Khan and B. Callan, *Int. J. Pharm.: X*, 2020, **2**, 100040.

160 M. Alibolandi, M. Ramezani, K. Abnous, F. Sadeghi and F. Hadizadeh, *J. Nanopart. Res.*, 2015, **17**, 76.

161 S. Kansiz and Y. M. Elcin, *Adv. Colloid Interface Sci.*, 2023, **317**, 102930.

162 S. W. Lee, M. H. Yun, S. W. Jeong, C. H. In, J. Y. Kim, M. H. Seo, C. M. Pai and S. O. Kim, *J. Controlled Release*, 2011, **155**, 262–271.

163 C. Oerlemans, W. Bult, M. Bos, G. Storm, J. F. Nijsen and W. E. Hennink, *Pharm. Res.*, 2010, **27**, 2569–2589.

164 R. Mundel, T. Thakur and M. Chatterjee, *3 Biotech*, 2022, **12**, 41.

165 N. Rostami, F. Faridghiasi, A. Ghebleh, H. Noei, M. Samadzadeh, M. M. Gomari, A. Tajiki, M. Abdouss, A. Aminoroaya, M. Kumari, R. Heidari, V. N. Uversky and B. R. Smith, *Polymers*, 2023, **15**, 3133.

166 T. Y. Wu, Z. L. Li, Y. C. Gong and X. Y. Xiong, *Nanomedicine*, 2023, **18**, 455–469.

167 L. Van Gheluwe, S. David, E. Buchy, I. Chourpa and E. Munnier, *Materials*, 2023, **16**, 539.

168 M. M. Allyn, R. H. Luo, E. B. Hellwarth and K. E. Swindle-Reilly, *Front. Med.*, 2021, **8**, 787644.

169 I. Chandrasiri, D. G. Abebe, M. Loku Yaddehige, J. S. D. Williams, M. F. Zia, A. Dorris, A. Barker, B. L. Simms, A. Parker, B. P. Vinjamuri, N. Le, J. N. Gayton, M. B. Chougule, N. I. Hammer, A. Flynt, J. H. Delcamp and D. L. Watkins, *ACS Appl. Bio Mater.*, 2020, **3**, 5664–5677.

170 X. Liu and H. Zhao, *Macromolecules*, 2024, **57**, 9677–9687.

171 M. Fonseca, I. Jarak, F. Victor, C. Domingues, F. Veiga and A. Figueiras, *Materials*, 2024, **17**, 319.

172 S. M. Carvalho, A. G. Leonel, A. A. P. Mansur, I. C. Carvalho, K. Krambrock and H. S. Mansur, *Biomater. Sci.*, 2019, **7**, 2102–2122.

173 M. Curcio, G. Cirillo, O. Vittorio, U. G. Spizzirri, F. Iemma and N. Picci, *Eur. Polym. J.*, 2015, **67**, 304–313.

